
Landscape of Thoughts: Visualizing the Reasoning Process of Large Language Models

Zhanke Zhou ^{1,2,*} Zhaocheng Zhu ^{3,4,*} Xuan Li ^{1,*} Mikhail Galkin ⁶
Xiao Feng ¹ Sanmi Koyejo ² Jian Tang ^{3,5} Bo Han ¹

Abstract

1 Numerous applications of large language models (LLMs) rely on their ability to
2 perform step-by-step reasoning. However, the reasoning behavior of LLMs remains
3 poorly understood, posing challenges to research, development, and safety. To
4 address this gap, we introduce *landscape of thoughts*-the first visualization tool for
5 users to inspect the reasoning paths of chain-of-thought and its derivatives on any
6 multi-choice dataset. Specifically, we represent the states in a reasoning path as
7 feature vectors that quantify their distances to all answer choices. These features are
8 then visualized in two-dimensional plots using t-SNE. Qualitative and quantitative
9 analysis with the landscape of thoughts effectively distinguishes between strong
10 and weak models, correct and incorrect answers, as well as different reasoning
11 tasks. It also uncovers undesirable reasoning patterns, such as low consistency and
12 high uncertainty. Additionally, users can adapt our tool to a model that predicts
13 the property they observe. We showcase this advantage by adapting our tool to a
14 lightweight verifier that evaluates the correctness of reasoning paths. Empirically,
15 this verifier boosts the accuracy of reasoning as well as the test-time scaling
16 effect. The code is publicly available at [https://github.com/tmlr-group/](https://github.com/tmlr-group/landscape-of-thoughts)
17 [landscape-of-thoughts](https://github.com/tmlr-group/landscape-of-thoughts).

18 1 Introduction

19 Large language models (LLMs) have revolutionized the paradigm of solving problems with their
20 broad spectrum of capabilities. In particular, several useful applications of LLMs, such as tool
21 use [37], retrieval-augmented generation [26], and agents [57], heavily rely on their capability of
22 step-by-step reasoning [53, 25]. Although many base models, *e.g.*, OpenAI o1 [19], and decoding
23 algorithms, *e.g.*, test-time scaling-up search [41], have been introduced to advance the performance
24 of LLMs on these applications, the underlying *reasoning behavior* of LLMs remains unclear to the
25 community. This hinders the development of algorithms and poses potential risks at deployment [4].

26 A few pioneer attempts [50, 35, 36, 11] have been made to understand the reasoning capacity of LLMs.
27 Nevertheless, these findings are often tied to certain decoding algorithms and problem-solving tasks,
28 which may not be so instructive for users working with their own algorithms and tasks. Instead, there
29 is a strong demand for such tools that can be applied to analyze the reasoning behavior of LLMs in
30 the users' scenarios. We foresee that such tools will at least benefit three groups of practitioners: First,
31 engineers can iterate their solutions faster based on the feedback from the tool; Second, reasoning
32 researchers can improve decoding algorithms based on insights revealed by the tool; And third, safety
33 researchers can utilize the tool to monitor, understand, and improve the behavior of LLMs.

34 We made a small but meaningful step towards the above goal by introducing the *landscape of*
35 *thoughts*, a tool for visualizing the reasoning paths produced by chain-of-thought and other step-

*Equal Contribution, ¹TMLR Group, Hong Kong Baptist University, ²Stanford University, ³Mila - Québec
AI Institute, ⁴Université de Montréal, ⁵HEC Montréal, ⁶Intel AI Lab.

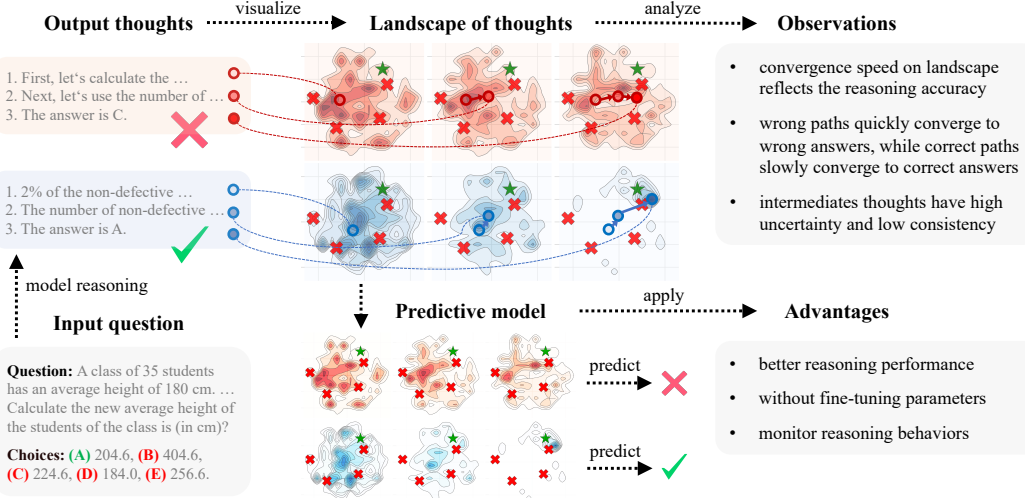


Figure 1: Landscape of thoughts for visualizing the reasoning steps of LLMs. Note that the red landscape represents wrong reasoning cases, while the blue indicates the correct ones. The darker regions in landscapes indicate more thoughts, with \times indicating incorrect answers and \star marking correct answers. Specifically, given a question with multiple choices, we sample a few thoughts from an LLM and divide them into two categories based on correctness. We visualize the landscape of each category by projecting the thoughts into a two-dimensional feature space, where each density map reflects the distribution of states at a reasoning step. With these landscapes, users can easily discover the reasoning patterns of an LLM or a decoding algorithm. In addition, a predictive model is applied to predict the correctness of landscapes and can help improve the accuracy of reasoning.

36 by-step reasoning algorithms. Given any multi-choice reasoning dataset, our tool visualizes the
 37 distribution of intermediate states and any reasoning path of interest *w.r.t.* the answer choices, which
 38 enables users to uncover reasoning patterns of LLMs in both success and failure cases (Fig. 1). The
 39 core idea is to characterize the textual states of thoughts in a reasoning path as features that quantify
 40 their distances to all answer choices. These distances are estimated by the commonly used perplexity
 41 metric, with the same LLM to generate thoughts and explain to itself. The state features are then
 42 projected to a two-dimensional space via t-SNE [49], a non-linear dimensionality reduction method
 43 to preserve manifolds in the original high-dimensional space, based on which the plots are drawn.

44 We examine our tool with different combinations of model sizes, decoding algorithms, and benchmark
 45 datasets. Our tool reveals several qualitative observations regarding the reasoning behaviors of LLMs.
 46 Some notable observations include: 1) The convergence speed of reasoning paths towards correct
 47 answers reflects the accuracy, no matter what base model, decoding algorithm, or dataset is used;
 48 2) The convergence speed of reasoning paths in success and failure cases is distinct, indicating that
 49 we may use the convergence speed of a reasoning path to predict its accuracy; 3) Low consistency
 50 and high uncertainty are generally observed in the intermediate thoughts, presenting the unstable
 51 properties of the reasoning process. To our knowledge, these observations have not been reported by
 52 previous works that analyze chain-of-thought mostly based on text analysis and performance metrics.

53 Since our tool is built on the top of state features, it can be adapted to a machine-learning model
 54 to quantitatively predict certain properties, such as the findings mentioned above. We showcase
 55 this advantage by training a lightweight model to predict the success and failure cases, which is
 56 equivalent to verifiers commonly used in LLM reasoning [8]. Even though this verifier is lightweight
 57 compared to most LLM-based verifiers, it consistently improves the reasoning performance on most
 58 combinations of models, decoding algorithms, and datasets in our experiments. Hence, users can
 59 further leverage this advantage to predict potential properties that they discover in their scenarios.

60 In summary, our main contributions are three-fold:

- 61 • We introduce the first visualization tool for inspecting the reasoning dynamics of different LLMs
 62 and decoding algorithms on any multi-choice reasoning dataset (Sec. 2).
- 63 • Our tool reveals several observations regarding the reasoning behaviors of different models,
 64 algorithms, and datasets, offering new insights into the reasoning (Sec. 3).

65 • Our tool can also be adapted to a model to predict certain properties and guide the reasoning
 66 process, improving LLM reasoning without modifying parameters (Sec. 4).

67 **2 Visualizing Multi-step Reasoning of LLMs**

68 This section outlines a general framework for language models and reasoning algorithms compatible
 69 with our tool (Sec. 2.1), demonstrates how it visualizes reasoning by projecting thoughts into a
 70 two-dimensional space (Sec. 2.2), and introduces metrics for quantitative analysis (Sec. 2.3).

71 **2.1 Problem Formulation**

72 Our goal is to *visualize* the reasoning process of LLMs across a variety of problem types. To achieve
 73 this, we aim for a formulation that is sufficiently general to encompass a wide range of use cases.
 74 Specifically, we focus on datasets consisting of multiple-choice questions, where each sample (x, y, \mathcal{C})
 75 comprises a question x , a correct answer y , and a finite set of candidate choices $\mathcal{C} = \{c_j\}_{j=1}^k$, all
 76 represented in texts. The visualization tool applies to the following models and algorithms.

77 **Language models.** To explore the landscape of thoughts generated by an LLM $p_{\text{LLM}}(\cdot)$, it is necessary
 78 for the model to produce diverse reasoning paths for solving a given problem. This requires the
 79 LLM to support sampling during inference $\hat{y} \sim p_{\text{LLM}}(y|x, \mathcal{C})$. For chain-of-thought reasoning,
 80 thoughts are sampled autoregressively as $\hat{t}_i \sim p_{\text{LLM}}(t_i|x, \mathcal{C}, \hat{t}_1, \dots, \hat{t}_{i-1})$. Namely, each thought
 81 \hat{t}_i is conditioned on the problem x , the candidate set \mathcal{C} , and the sequence of preceding thoughts
 82 $\hat{t}_1, \dots, \hat{t}_{i-1}$. To characterize intermediate states within these reasoning paths, the LLM must also
 83 function as a likelihood estimator, enabling the computation of the probability $p_{\text{LLM}}(\hat{y}|x, \mathcal{C}, \hat{t}_1, \dots, \hat{t}_i)$
 84 of any generation \hat{y} . These two requirements are generally satisfied by most open-source LLMs, such
 85 as Llama [10], Mistral [20], and DeepSeek [29]. However, proprietary LLMs, such as GPT-4 [1] and
 86 Gemini [45], are excluded as they do not support likelihood estimation with the logits of generations.

87 **Reasoning algorithms.** While there are many approaches to solving reasoning problems with
 88 LLMs [9, 22], this work focuses on chain-of-thought (CoT) [53] and its derivatives [62, 56], owing
 89 to their widespread use and development. These decoding algorithms generally guide the model in
 90 generating a structured path of intermediate reasoning thoughts before arriving at the final answer.
 91 Note that to visualize a large number of reasoning thoughts effectively, these thoughts should be
 92 automatically parsed into distinct units (e.g., via sentence tokenization). This requirement is typically
 93 satisfied by most variants of CoT. We also empirically verify the robustness of our tool if this
 94 requirement does not hold (please see Appendix D.2 for detailed experiments).

95 **2.2 Landscape of Thoughts**

96 Given a collection of reasoning paths generated by an LLM, our tool seeks to visualize how different
 97 paths lead to either correct or incorrect answers within a two-dimensional (2D) space, as illustrated
 98 in Fig. 1. A key challenge lies in the absence of a direct mapping from the textual space of thoughts
 99 to 2D coordinates. To address this gap, we first utilize the same LLM to represent intermediate states
 100 as numerical vectors. These state vectors are then projected into a 2D space for visualization. For
 101 simplicity, we use the notation t_i instead of \hat{t}_i , which is clear in the following.

102 **Characterizing the states.** Here, the intermediate *thoughts* $\{t_i\}_{i=1}^n$ in a reasoning path naturally
 103 define a sequence of *states* $\{s_i\}_{i=0}^n$, where $s_0 = [x]$ and $s_i = [x, t_1, t_2, \dots, t_i]$. Here, we propose to
 104 characterize the states as feature vectors using the likelihood function of the LLM. Specifically, the
 105 k -dim feature vector s_i for state s_i is defined as follows:

$$s_i = [d(s_i, c_1), d(s_i, c_2), \dots, d(s_i, c_k)]^\top, \quad (1)$$

106 where $d(s_i, c_j)$ measures the *distance* between state s_i and choice c_j . Here, the vector s_i indicates
 107 the relative distances from the state s_i to all possible choices $\{c_j\}_{j=1}^k$. To reduce the effect of length
 108 on choices, we calculate the distance of $d(s_i, c_j)$ through the perplexity metric [38, 32]:²

$$d(s_i, c_j) = p_{\text{LLM}}(c_j|s_i)^{-1/|c_j|}, \quad (2)$$

²The perplexity can also be expressed as $\text{PPL}(c_j|s_i) = \exp\left(-\frac{1}{|c_j|} \sum_{t=1}^{|c_j|} \log p_{\text{LLM}}(c_j[t]|s_i, c_j[:t])\right)$.

109 where $|c_j|$ is the number of tokens in c_j , and $p_{\text{LLM}}(c_j|s_i)$ is the accumulated probability in an autoregressive manner. We further normalize the vector s_i to have a unit L1 normalization. Additionally, 110 to represent the choices as landmarks in the visualization, it is necessary to encode the choices as 111 feature vectors. Notably, the perplexity decreases as the model’s prediction confidence increases. To 112 align with this observation, we define the feature vector c_j for a choice c_j as: 113

$$c_j = \frac{1}{k} [\mathbb{1}(j \neq 1), \dots, \mathbb{1}(j \neq k)]^\top. \quad (3)$$

114 For r paths, each with n states, we compute the feature vectors for all $r \cdot n$ states.³ Together with the 115 feature vectors of k choices, we obtain a feature matrix $S \in \mathbb{R}^{k \times (r \cdot n + k)}$ as:

$$S = [s_1^{(1)}, \dots, s_n^{(1)}, \dots, s_1^{(r)}, \dots, s_n^{(r)}, c_1, \dots, c_k]. \quad (4)$$

116 Note that a sufficiently large number of paths is necessary to generate a comprehensive visualization 117 of the reasoning landscape. However, visualizing all samples in a dataset under this setting incurs 118 a significant computational cost. In practice, we found it more efficient to visualize d paths with $\frac{r}{d}$ 119 samples projected into the same space. This approach retains much of the visualization quality while 120 substantially reducing the number of paths required for each sample. The key idea is to rearrange 121 the order of choices such that the correct answer consistently aligns with the same dimension in the 122 k -dimensional feature space across all the r samples. 123

Visualization. After constructing the feature matrix S , we project the states and choices into a 124 2D space for visualization. This dimensionality reduction step can be accomplished using various 125 existing algorithms [34, 49, 33]. In this study, we employ t-SNE [49] due to its ability to preserve the 126 underlying manifolds of the original high-dimensional space and its robustness to a wide range of 127 transformations. By applying t-SNE to the k -dim S , we obtain the 2-dim coordinates $\tilde{S} \in \mathbb{R}^{2 \times (rn+k)}$. 128 The two axes in the landscape visualization correspond to reduced dimensions from the original 129 spaces. This original space captures the full answer space for problem-solving, with each state’s 130 coordinates reflecting its relative distance to different answers. The coordinates of the states define 131 a discrete density function in the 2D space. To create a more intuitive and visually interpretable 132 representation, we smooth this density function using a Parzen window estimator [40]. The smoothed 133 density at a given coordinate \bar{v} is as follows, where the σ controls the radius of Gaussian kernels:

$$p(\bar{v}) = \frac{1}{rn} \sum_{\bar{s} \in \tilde{S}} \exp \left(-\frac{\|\bar{v} - \bar{s}\|^2}{2\sigma^2} \right). \quad (5)$$

134 2.3 Metrics

135 Besides the qualitative visualization, we introduce three quantitative metrics to help understand the 136 LLMs’ behavior. These metrics are defined based on the intermediate states in Sec. 2.2.

137 **Consistency.** To understand whether the LLM knows the answer before generating all thoughts, we 138 compute the consistency of state s_i by checking whether s_i and s_n agree

$$\text{Consistency}(s_i) = \mathbb{1}(\arg \min s_i = \arg \min s_n). \quad (6)$$

139 **Uncertainty.** To know how confident the LLM is about its predictions at intermediate steps, we 140 compute the uncertainty of state s_i as the entropy of s_i (note $\sum_{d \in s_i} d = 1$)

$$\text{Uncertainty}(s_i) = - \sum_{d \in s_i} d \cdot \log d. \quad (7)$$

141 **Perplexity.** We are also interested in how confident the LLM is about its thoughts. We use the 142 perplexity of thought t_i , since it is comparable across thoughts of different length

$$\text{Perplexity}(t_i) = p_{\text{LLM}}(t_i|s_{i-1})^{-1/|t_i|}. \quad (8)$$

143 3 Results and Observations

144 In this section, we utilize the landscape of thoughts to analyze the reasoning behavior of LLMs. 145 Specifically, we conduct a comprehensive evaluation and extract several observations by comparing

³Our tool can also be applied to paths with different numbers of states. We assume n states for demonstrations.

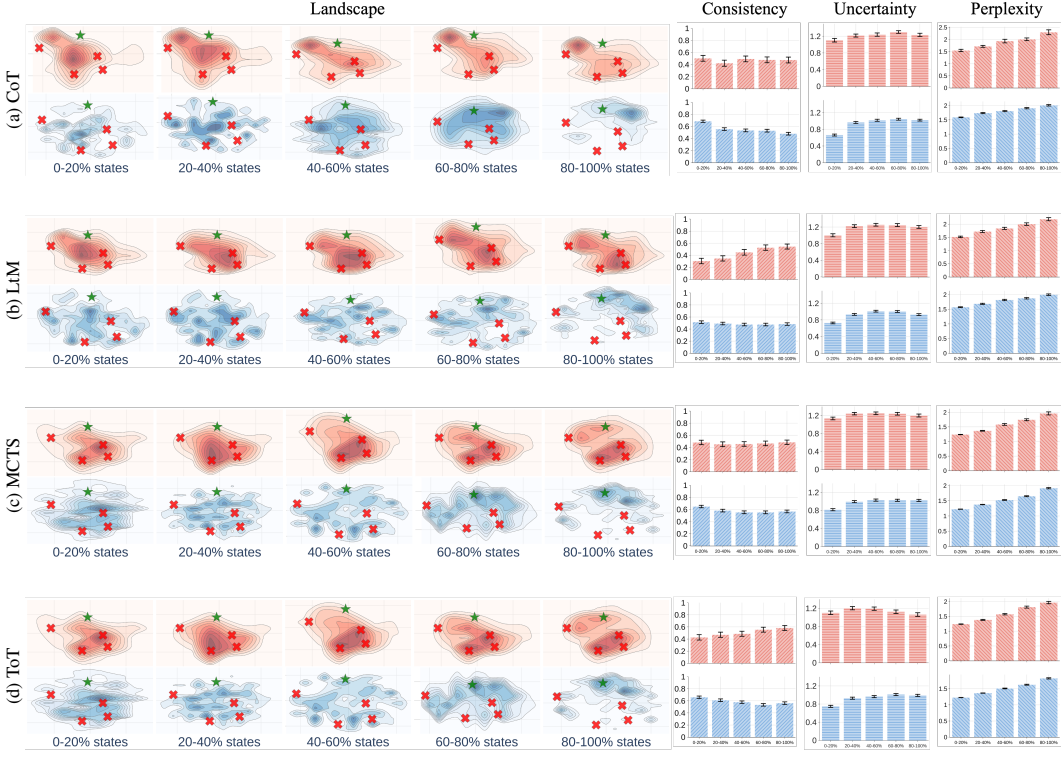


Figure 2: Comparing the landscapes and corresponding metrics of four reasoning algorithms (using Llama-3.1-70B on the AQuA dataset). Through the reasoning progression, spanning from early (0-20% states) to the later stages (80-100% states), the visualization shows correct cases (bottom row in blue) with incorrect cases (top row in red). Metrics are calculated *w.r.t.* each bin, *e.g.*, 20% - 40% of states. Note that darker regions represent a higher density of states, with \times indicating incorrect answers and \star marking correct answers. The accuracy of reasoning for the four subfigures is: (a) 84.4%, (b) 82.2%, (c) 75.8%, and (d) 81.6%, respectively.

146 the landscape of thoughts across three dimensions: (1) various *reasoning algorithms* in Sec. 3.1, (2)
 147 different *reasoning tasks* in Sec. 3.2, and (3) diverse scales of *language models* in Sec. 3.3.
 148 To help understand the qualitative visualizations, we quantitatively calculate the consistency and
 149 uncertainty of states, as well as the perplexity of thoughts, all previously introduced in Sec. 2.3. Unless
 150 stated otherwise, we employ Llama-3.1-70B with CoT as the default configuration in evaluations.
 151 Note that all the visualizations are built upon the model’s estimation of their intermediate thoughts.

152 3.1 Comparison across Reasoning Algorithms

153 **Setup.** We evaluate the default model with four reasoning algorithms: chain-of-thought (CoT) [53],
 154 least-to-most (LtM) [62], MCTS [61], and tree-of-thought (ToT) [56]. We run these algorithms on 50
 155 problems randomly selected from the AQuA dataset. The corresponding landscapes are presented in
 156 Fig. 2, which yields the following observations. Further discussion, detailed experimental settings,
 157 and additional results can be found in Appendix B, C, and D, respectively.

158 **Observation 3.1** (*The landscapes converge faster to the correct answers are of higher reasoning*
 159 *accuracy*). By comparing the four groups of landscapes in Fig. 2, we observe that the states scatter
 160 dispersedly at early stages and gradually converge to correct (or incorrect) answers in later stages.
 161 Here, converge means the trend of a reasoning path approaching one answer. As can be seen from
 162 Fig. 2, different reasoning algorithms present diverse landscapes. Generally, methods with more
 163 scattered landscapes (converge slower) present lower accuracy than those that converge faster.

164 **Observation 3.2** (*Wrong paths quickly converge to wrong answers, while correct paths slowly step*
 165 *to correct answers*). By comparing the landscapes of failure and success paths, it is found that the
 166 failure paths usually converge to the wrong answers at earlier states of reasoning, *e.g.*, 20-40% states.
 167 By contrast, the states in the success paths converge to the correct answers at later 80-100% states.

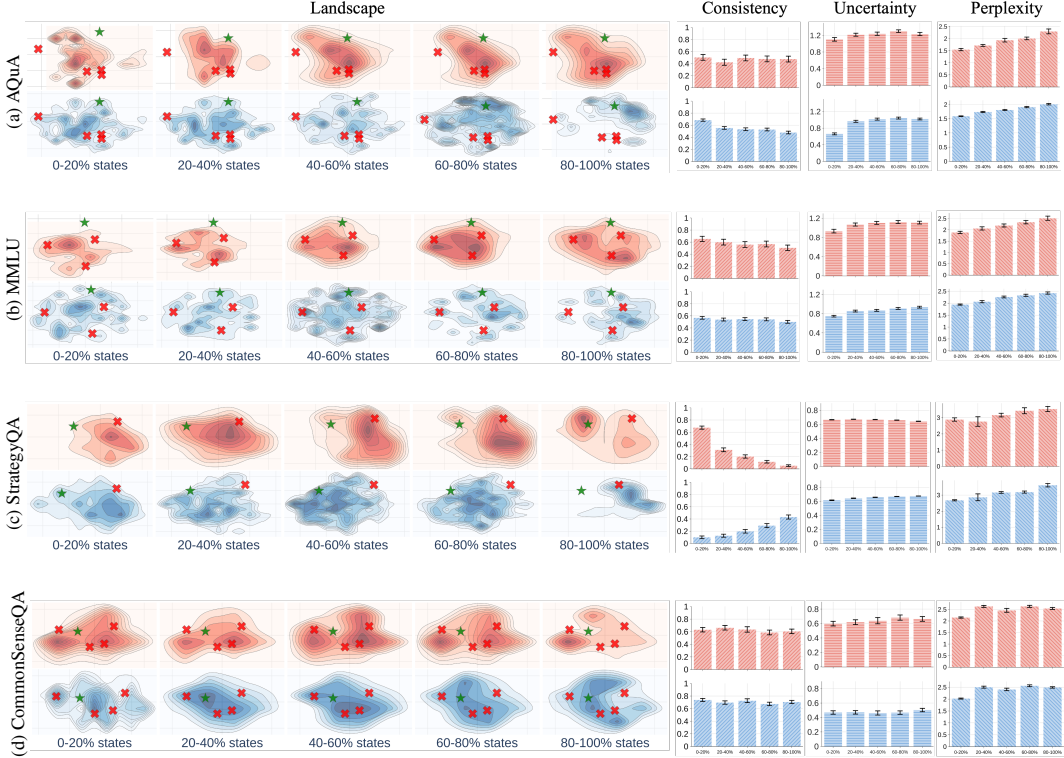


Figure 3: Comparing the landscapes and corresponding metrics of different datasets (using Llama-3.1-70B with CoT). Darker regions represent higher state density, with x indicating incorrect answers and \star marking the correct ones. In addition, the accuracy of reasoning for the four subfigures is: (a) 84.4%, (b) 80.2%, (c) 75.8%, and (d) 64.8%, respectively.

168 This implies that early states of the reasoning process can lead to any potential answers (from model
169 perspective), while the correct answers are usually determined at the end of reasoning paths.

170 **Observation 3.3** (*Compared to failure paths, the intermediate states in correct paths have higher
171 consistency w.r.t. the final state*). By comparing the consistency plots in Fig. 2, we found that the
172 model generally has low consistency between the intermediate states and the final state. Notably, the
173 consistency of wrong paths is significantly lower than that of correct paths. This implies that the
174 reasoning process can be quite unstable. Even though decoding algorithms like CoT and LtM are
175 designed to solve a problem directly (without explorations), the generated thoughts by these methods
176 do not consistently guide the reasoning path to the answer.

177 3.2 Comparison across Reasoning Tasks

178 **Setup.** Besides the AQuA, we include MMLU, CommonsenseQA, and StrategyQA datasets. We run
179 the base model with CoT on 50 problems per dataset. The observations follow are derived from the
180 landscapes in Fig. 3. More visualization cases can be found in Appendix E.

181 **Observation 3.4** (*Similar reasoning tasks exhibit similar landscapes*). The landscapes of AQuA,
182 MMLU, and StrategyQA exhibit organized search behavior with higher state diversity, while Com-
183 monSenseQA presents concentrated search regions, reflecting direct knowledge retrieval rather than
184 step-by-step reasoning processes. These distinct landscape patterns demonstrate the potential to
185 reveal underlying domain relationships across different reasoning tasks.

186 **Observation 3.5** (*Different reasoning tasks present significantly different patterns in consistency,
187 uncertainty, and perplexity*). The histograms in Fig. 3 show that path perplexity consistently increases
188 as reasoning progresses across all datasets. Specifically, different datasets, *e.g.*, AQuA and MMLU,
189 show distinctly higher levels of uncertainty. As for StrategyQA, correct paths show increasing
190 consistency that surpasses incorrect paths at around 60% states, while incorrect paths show decreasing
191 consistency. However, extending beyond the typical three-step requirement [13], the later stages
192 (60-100% states) show increasing perplexity as well as lower uncertainty.

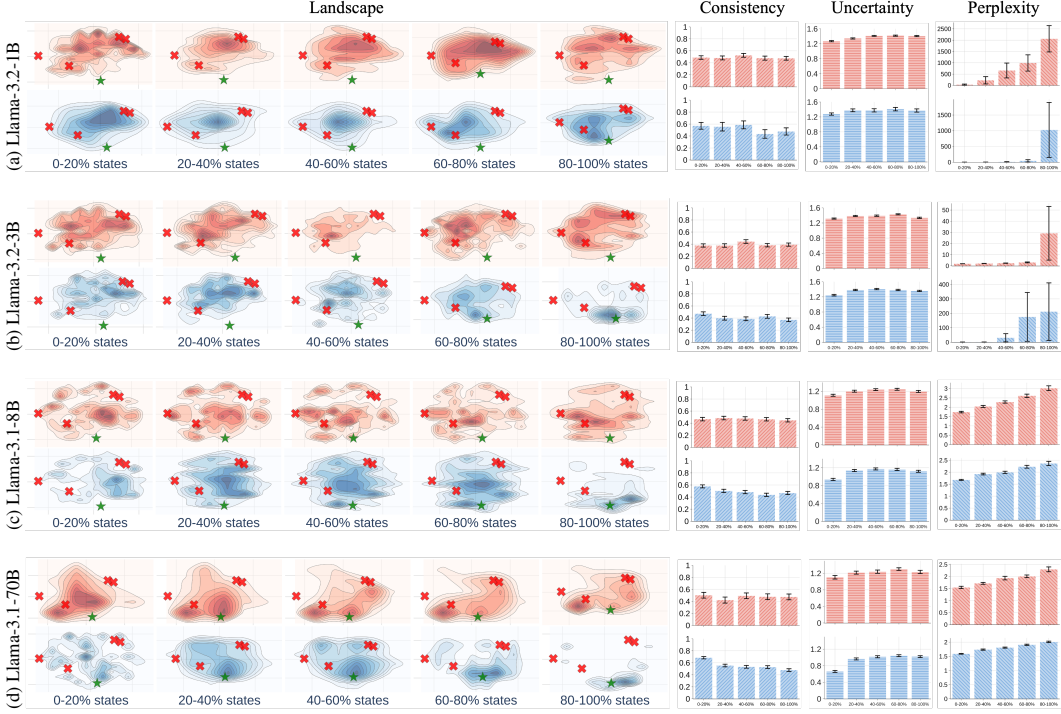


Figure 4: Comparing the landscapes and corresponding metrics of different language models (with CoT on the AQuA dataset). Darker regions represent higher state density, with \times indicating incorrect answers and \star marking the correct ones. In addition, the accuracy of reasoning for the four subfigures is: (a) 15.8%, (b) 42.0%, (c) 53.2%, and (d) 84.4%, respectively.

193 3.3 Comparison across Language Models

194 **Setup.** In this part, we study several LLMs’ behavior across different parameter scales (1B, 3B, 8B,
 195 and 70B). We run each model with CoT on 50 problems from the AQuA dataset. The landscapes of
 196 these models are shown in Fig. 4. We also provide case studies on the up-to-date reasoning models [14,
 197 46] in the Appendix E, whose behaviors are also consistent with the following observations.

198 **Observation 3.6** (*The landscape converges faster as the model size increase*). As model parameters
 199 scale from 1B to 70B, the corresponding landscape demonstrates faster convergence to the correct
 200 answers with higher density in the last 20% states, aligning with the increasing accuracy. With more
 201 parameters to store information, larger models can access broader knowledge [3]. This leads to more
 202 confident solutions, demonstrated by more focused answer patterns and lower uncertainty.

203 **Observation 3.7** (*Larger models have higher consistency, lower uncertainty, and lower perplexity*).
 204 As the model size increases, the consistency increases, at the same time, the uncertainty and perplexity
 205 decrease significantly. This also aligns with the higher accuracy for the large models.

206 4 Adapting Visualization to Predictive Models

207 One advantage of our method is that it can be adapted to a model to predict any property users
 208 observe. Here, we show how to convert our method to a lightweight verifier for voting reasoning
 209 paths, following the observations in Sec. 3. Note that this methodology is not limited to verifiers.
 210 Users can use this technique to adapt the visualization tool to monitor the properties in their scenarios.

211 4.1 A Lightweight Verifier

212 Observation 3.2 and 3.3 show that the convergence speed and consistency of intermediate states
 213 can distinguish correct and wrong paths. Inspired by these observations, we build a model f :
 214 $\mathbb{R}^{(k+1) \times n} \rightarrow \{0, 1\}$ to predict the correctness of a reasoning path based on the state features $\{s_i\}_{i=1}^n$
 215 and consistency metric $\{\text{Consistency}(s_i)\}_{i=1}^n$. The insight is that the state features, used to compute

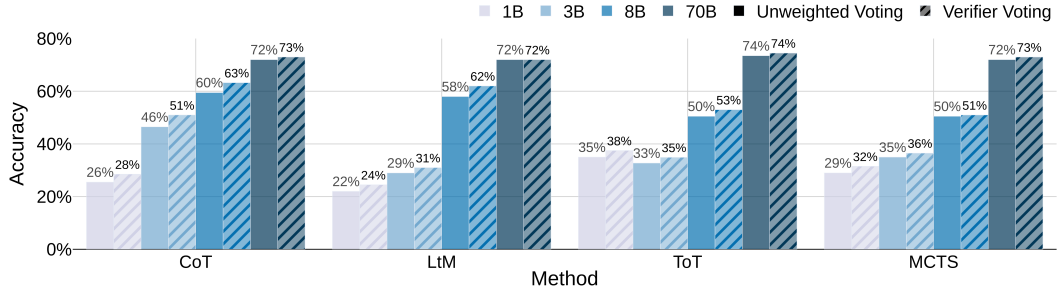


Figure 5: The accuracy of reasoning under different decoding methods and model scales (averaging across all four datasets). Results for each dataset are in Appendix E.

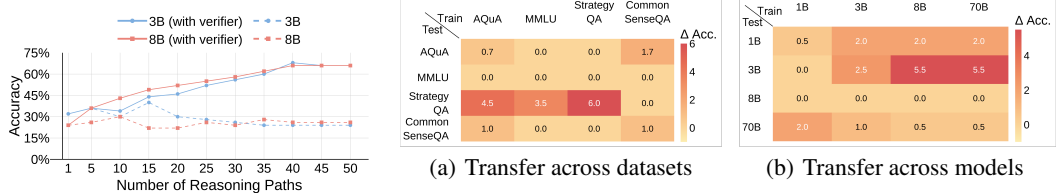


Figure 6: Demonstration of the inference-time scaling effect of the verifier. We show the voting accuracy (%) on StrategyQA scales with the number of reasoning paths.

Figure 7: Absolute accuracy changes (Δ Acc.) with the verifier, compared to performance in Fig. 5 (without the verifier). The verifier is trained on each column (dataset or model) and evaluated on all rows (other datasets or models). Positive values indicate improvement in accuracy with the verifier.

216 the 2-D visualization, encode rich location information of the states and can be used to estimate the
 217 convergence speed. Due to the small dimensionality of these features, we parameterize f with a
 218 random forest [5] to avoid overfitting. We use this model as a verifier to enhance LLM reasoning [8].
 219 Unlike popular verifiers [27] that involve a moderately sized language model on textual thoughts, our
 220 verifier operates on state features and is quite lightweight. We train a verifier on thoughts sampled
 221 on the training split of each dataset and apply it to vote reasoning paths at test time. Given q paths
 222 sampled by a decoding algorithm, the final prediction is produced by a weighted majority voting:

$$\hat{y} = \arg \max_{c \in \mathcal{C}} \sum_{i=1}^q \mathbb{1}(\hat{y}^{(i)} = c) \cdot f(\{s_i\}_{i=1}^n, \{\text{Consistency}(s_i)\}_{i=1}^n). \quad (9)$$

223 4.2 Experimental Results

224 We evaluate our numerical verifier against an unweighted voting baseline [52] with various models,
 225 decoding algorithms, and reasoning datasets. Detailed settings and results are in Appendix C.1.

226 **Effectiveness of the verifier.** We first compare our verifier against the unweighted voting baseline,
 227 each applied to 10 reasoning paths. As shown in Fig. 5, our verifier consistently enhances the
 228 reasoning performance of all models and decoding algorithms, even though our verifier does not use
 229 any pre-trained language model. Notably, smaller language models (1B and 3B) show significant
 230 performance gains with the verifier’s assistance, achieving substantial improvements over their
 231 original capabilities of reasoning. We also compare the verifier between reward-guided algorithms

232 **Test-time scaling.** While the improvement of the verifier seems marginal with 10 reasoning paths,
 233 our verifier can provide a substantial performance gain with more reasoning paths. We adjust the
 234 number of reasoning paths from 1 to 50, and plot the results of the verifier and the unweighted voting
 235 baseline in Fig. 6. Models with our verifier exhibit significantly stronger scaling behaviors, achieving
 236 over 65% accuracy. In contrast, the performance of the baseline saturated around 30% accuracy.
 237 These results suggest that our state features, which are used in both the visualization tool and the
 238 verifier, capture important information about the reasoning behavior of LLMs. Thus, the verifier can
 239 boost test-time scaling, especially in solving complex problems.

240 **Cross-dataset and cross-model transferability.** One interesting property of the state features and
 241 metrics is that their shape and range are agnostic to the model and dataset, suggesting that we may

242 deploy the verifier trained on one dataset or model in another setting. As illustrated in Fig. 7, we
243 evaluate how the verifier transfers across reasoning datasets (*e.g.*, train on AQuA and test on MMLU)
244 and model scales (*e.g.*, train on 1B model and test on 70B model). We observe some positive transfers
245 across datasets and models. For example, a verifier trained on AQuA can improve the performance
246 of StrategyQA by 4.5%. A verifier trained on the 70B model also improves the performance of the
247 3B model by 5.5%. However, some cases do not benefit from the transferring verifiers. We leave
248 improving the transferability of the state features and metrics as future work.

249 5 Related Work

250 **Reasoning with large language models.** Chain-of-Thought (CoT) prompting [53, 25] has empow-
251 ered LLMs to tackle multi-step reasoning problems by generating intermediate steps before producing
252 a final answer. Building upon CoT, numerous methods have been proposed to address various chal-
253 lenges, including compositional generalization [62, 23], planning [56, 15], and rule learning [63]
254 within the CoT reasoning. Beyond solving reasoning tasks, CoT has also emerged as a foundational
255 framework for other techniques, such as fine-tuning LLMs [60], enabling LLM-based agents [57],
256 and facilitating test-time scaling [41]. Nevertheless, most of these approaches are developed in a
257 trial-and-error manner, largely due to the absence of proper tools for analyzing the CoT.

258 **Understanding chain-of-thought reasoning.** There are a few studies that explore what makes
259 CoT prompting effective by perturbing its exemplars. To be specific, Madaan and Yazdanbakhsh
260 [31] found that the text and patterns of exemplars help CoT generate sentences resembling correct
261 answers. Besides, Wang et al. [50] highlighted the importance of maintaining the correct order
262 of reasoning steps, while Ye et al. [59] demonstrated that using complementary exemplars can
263 enhance reasoning performance. Furthermore, CoT can benefit from longer reasoning chains, even
264 without new information to the prompt [21]. Another line of research investigates CoT’s general
265 behavior [44, 35, 36, 39]. For example, CoT heavily depends on the semantic structure of the problem
266 to perform reasoning [44], struggles with planning and unification in deductive reasoning [35],
267 has difficulty generalizing to longer reasoning paths [36], and can be easily misled by irrelevant
268 information in the context [39]. However, these observations are derived from specific reasoning
269 tasks and prompt settings, limiting their applicability to other scenarios. In contrast, we introduce a
270 general-purpose tool that allows users to analyze reasoning in their contexts.

271 **Tools for analyzing chain-of-thought.** To the best of our knowledge, the only existing tool for
272 analyzing CoT is gradient-based feature attribution [54], which computes a saliency score for each
273 input token based on the model’s output. However, these token-level saliency scores do not directly
274 capture the thought-level, multi-step reasoning process of LLMs. Consequently, the main finding
275 in [54] is that CoT stabilizes saliency scores on semantically relevant tokens compared to direct
276 prompting. Metrics designed to quantify CoT performance [6, 48] can also be used to analyze the
277 reasoning behaviors of LLMs. For instance, Ton et al. [48] employs information gain to identify
278 failure modes in reasoning paths, aligning with Observation 3.2 in this paper. However, our 2-D
279 visualization offers significantly deeper insights than a single information gain metric. Additionally,
280 the verifier derived from our tool is conceptually related to outcome-supervised reward models [8].

281 6 Conclusion

282 This paper introduces the landscape of thoughts, a visualization tool for analyzing the reasoning
283 paths produced by large language models with chain-of-thought. Built on top of feature vectors
284 of intermediate states in reasoning paths, our tool reveals several insights into LLM reasoning,
285 such as the relationship between convergence and accuracy, and issues of low consistency and high
286 uncertainty. Our tool can also be adapted to predict the observed property, which is demonstrated by
287 a lightweight verifier developed based on the feature vectors and our observations. We foresee that
288 this tool will create several opportunities to develop, understand, and monitor the LLM reasoning.

289 One limitation of the landscape of thoughts is its applicability only to multiple-choice tasks. Future
290 work could focus on adapting this tool for open-ended reasoning tasks, such as mathematical problem-
291 solving, code generation, and planning, where reasoning paths are less structured and more complex.
292 Additionally, further research could aim to make the tool more accessible by generating intuitive
293 visual and textual explanations, enabling non-experts to better understand and trust the reasoning
294 processes of LLMs. Another promising direction is the development of automated methods to detect
295 reasoning failures at scale, which could enhance the reliability of LLMs across diverse applications.

296 **References**

297 [1] Josh Achiam, Steven Adler, Sandhini Agarwal, Lama Ahmad, Ilge Akkaya, Florencia Leoni
298 Aleman, Diogo Almeida, Janko Altenschmidt, Sam Altman, Shyamal Anadkat, et al. Gpt-4
299 technical report. *arXiv preprint arXiv:2303.08774*, 2023.

300 [2] Guillaume Alain and Yoshua Bengio. Understanding intermediate layers using linear classifier
301 probes. *arXiv preprint arXiv:1610.01644*, 2016.

302 [3] Zeyuan Allen-Zhu and Yuanzhi Li. Physics of language models: Part 3.3, knowledge capacity
303 scaling laws. *arXiv preprint arXiv:2404.05405*, 2024.

304 [4] Usman Anwar, Abulhair Saparov, Javier Rando, Daniel Paleka, Miles Turpin, Peter Hase,
305 Ekdeep Singh Lubana, Erik Jenner, Stephen Casper, Oliver Sourbut, et al. Foundational
306 challenges in assuring alignment and safety of large language models. *TMLR*, 2024.

307 [5] Leo Breiman. Random forests. *Machine learning*, 2001.

308 [6] Qiguang Chen, Libo Qin, Jiaqi Wang, Jinxuan Zhou, and Wanxiang Che. Unlocking the
309 capabilities of thought: A reasoning boundary framework to quantify and optimize chain-of-
310 thought. In *NeurIPS*, 2024.

311 [7] Kevin Clark, Urvashi Khandelwal, Omer Levy, and Christopher D. Manning. What does bert
312 look at? an analysis of bert’s attention. In *ACL Workshop BlackboxNLP*, 2019.

313 [8] Karl Cobbe, Vineet Kosaraju, Mohammad Bavarian, Mark Chen, Heewoo Jun, Lukasz Kaiser,
314 Matthias Plappert, Jerry Tworek, Jacob Hilton, Reiichiro Nakano, et al. Training verifiers to
315 solve math word problems. *arXiv preprint arXiv:2110.14168*, 2021.

316 [9] Antonia Creswell, Murray Shanahan, and Irina Higgins. Selection-inference: Exploiting large
317 language models for interpretable logical reasoning. *arXiv preprint arXiv:2205.09712*, 2022.

318 [10] Abhimanyu Dubey, Abhinav Jauhri, Abhinav Pandey, Abhishek Kadian, Ahmad Al-Dahle,
319 Aiesha Letman, Akhil Mathur, Alan Schelten, Amy Yang, Angela Fan, et al. The llama 3 herd
320 of models. *arXiv preprint arXiv:2407.21783*, 2024.

321 [11] Nouha Dziri, Ximing Lu, Melanie Sclar, Xiang Lorraine Li, Liwei Jiang, Bill Yuchen Lin, Sean
322 Welleck, Peter West, Chandra Bhagavatula, Ronan Le Bras, et al. Faith and fate: Limits of
323 transformers on compositionality. In *NeurIPS*, 2024.

324 [12] Nelson Elhage, Neel Nanda, Catherine Olsson, Tom Henighan, Nicholas Joseph, Ben Mann,
325 Amanda Askell, Yuntao Bai, Anna Chen, Tom Conerly, et al. A mathematical framework for
326 transformer circuits. *Transformer Circuits Thread*, 2021.

327 [13] Mor Geva, Daniel Khashabi, Elad Segal, Tushar Khot, Dan Roth, and Jonathan Berant. Did
328 aristotle use a laptop? a question answering benchmark with implicit reasoning strategies.
329 *TACL*, 2021.

330 [14] Daya Guo, Dejian Yang, Haowei Zhang, Junxiao Song, Ruoyu Zhang, Runxin Xu, Qihao Zhu,
331 Shirong Ma, Peiyi Wang, Xiao Bi, et al. Deepseek-r1: Incentivizing reasoning capability in
332 llms via reinforcement learning. In *arXiv*, 2025.

333 [15] Shibo Hao, Yi Gu, Haodi Ma, Joshua Hong, Zhen Wang, Daisy Wang, and Zhiting Hu.
334 Reasoning with language model is planning with world model. In *EMNLP*, 2023.

335 [16] Dan Hendrycks, Collin Burns, Steven Basart, Andy Zou, Mantas Mazeika, Dawn Song, and
336 Jacob Steinhardt. Measuring massive multitask language understanding. In *ICLR*, 2021.

337 [17] John Hewitt and Percy Liang. Designing and interpreting probes with control tasks. In *EMNLP*,
338 2019.

339 [18] Daphne Ippolito, Florian Tramèr, Milad Nasr, Chiyuan Zhang, Matthew Jagielski, Katherine
340 Lee, Christopher A Choquette-Choo, and Nicholas Carlini. Preventing verbatim memorization
341 in language models gives a false sense of privacy. *arXiv preprint arXiv:2210.17546*, 2022.

342 [19] Aaron Jaech, Adam Kalai, Adam Lerer, Adam Richardson, Ahmed El-Kishky, Aiden Low, Alec
343 Helyar, Aleksander Madry, Alex Beutel, Alex Carney, et al. Openai o1 system card. *arXiv*
344 *preprint arXiv:2412.16720*, 2024.

345 [20] Albert Q Jiang, Alexandre Sablayrolles, Antoine Roux, Arthur Mensch, Blanche Savary, Chris
346 Bamford, Devendra Singh Chaplot, Diego de las Casas, Emma Bou Hanna, Florian Bressand,
347 et al. Mixtral of experts. *arXiv preprint arXiv:2401.04088*, 2024.

348 [21] Mingyu Jin, Qinkai Yu, Dong Shu, Haiyan Zhao, Wenyue Hua, Yanda Meng, Yongfeng Zhang,
349 and Mengnan Du. The impact of reasoning step length on large language models. *arXiv preprint*
350 *arXiv:2401.04925*, 2024.

351 [22] Mehran Kazemi, Najoung Kim, Deepti Bhatia, Xin Xu, and Deepak Ramachandran. Lambada:
352 Backward chaining for automated reasoning in natural language. In *ACL*, 2023.

353 [23] Tushar Khot, Harsh Trivedi, Matthew Finlayson, Yao Fu, Kyle Richardson, Peter Clark, and
354 Ashish Sabharwal. Decomposed prompting: A modular approach for solving complex tasks. In
355 *ICLR*, 2023.

356 [24] Goro Kobayashi, Tatsuki Kuribayashi, Sho Yokoi, and Kentaro Inui. Attention is not only a
357 weight: Analyzing transformers with vector norms. In *EMNLP*, 2020.

358 [25] Takeshi Kojima, Shixiang Shane Gu, Machel Reid, Yutaka Matsuo, and Yusuke Iwasawa. Large
359 language models are zero-shot reasoners. In *NeurIPS*, 2022.

360 [26] Patrick Lewis, Ethan Perez, Aleksandra Piktus, Fabio Petroni, Vladimir Karpukhin, Naman
361 Goyal, Heinrich Kütter, Mike Lewis, Wen-tau Yih, Tim Rocktäschel, et al. Retrieval-augmented
362 generation for knowledge-intensive nlp tasks. In *NeurIPS*, 2020.

363 [27] Hunter Lightman, Vineet Kosaraju, Yura Burda, Harri Edwards, Bowen Baker, Teddy Lee, Jan
364 Leike, John Schulman, Ilya Sutskever, and Karl Cobbe. Let’s verify step by step. *arXiv preprint*
365 *arXiv:2305.20050*, 2023.

366 [28] Wang Ling, Dani Yogatama, Chris Dyer, and Phil Blunsom. Program induction by rationale
367 generation: Learning to solve and explain algebraic word problems. In *ACL*, 2017.

368 [29] Aixin Liu, Bei Feng, Bing Xue, Bingxuan Wang, Bochao Wu, Chengda Lu, Chenggang Zhao,
369 Chengqi Deng, Chenyu Zhang, Chong Ruan, et al. Deepseek-v3 technical report. *arXiv preprint*
370 *arXiv:2412.19437*, 2024.

371 [30] Liangchen Luo, Yinxiao Liu, Rosanne Liu, Samrat Phatale, Meiqi Guo, Harsh Lara, Yunxuan
372 Li, Lei Shu, Yun Zhu, Lei Meng, et al. Improve mathematical reasoning in language models by
373 automated process supervision. In *arXiv*, 2024.

374 [31] Aman Madaan and Amir Yazdanbakhsh. Text and patterns: For effective chain of thought, it
375 takes two to tango. *arXiv preprint arXiv:2209.07686*, 2022.

376 [32] C. Manning. *Foundations of statistical natural language processing*. The MIT Press, 1999.

377 [33] Leland McInnes, John Healy, and James Melville. Umap: Uniform manifold approximation
378 and projection for dimension reduction. *arXiv preprint arXiv:1802.03426*, 2018.

379 [34] Karl Pearson. Liii. on lines and planes of closest fit to systems of points in space. *The London,*
380 *Edinburgh, and Dublin philosophical magazine and journal of science*, 1901.

381 [35] Abulhair Saparov and He He. Language models are greedy reasoners: A systematic formal
382 analysis of chain-of-thought. In *ICLR*, 2023.

383 [36] Abulhair Saparov, Richard Yuanzhe Pang, Vishakh Padmakumar, Nitish Joshi, Mehran Kazemi,
384 Najoung Kim, and He He. Testing the general deductive reasoning capacity of large language
385 models using ood examples. In *NeurIPS*, 2023.

386 [37] Timo Schick, Jane Dwivedi-Yu, Roberto Dessì, Roberta Raileanu, Maria Lomeli, Eric Hambro,
 387 Luke Zettlemoyer, Nicola Cancedda, and Thomas Scialom. Toolformer: Language models can
 388 teach themselves to use tools. In *NeurIPS*, 2023.

389 [38] C. E. Shannon. A mathematical theory of communication. *The Bell System Technical Journal*,
 390 1948.

391 [39] Freda Shi, Xinyun Chen, Kanishka Misra, Nathan Scales, David Dohan, Ed Chi, Nathanael
 392 Schärli, and Denny Zhou. Large language models can be easily distracted by irrelevant context.
 393 In *ICML*, 2023.

394 [40] Bernard W Silverman. *Density estimation for statistics and data analysis*. Routledge, 2018.

395 [41] Charlie Snell, Jaehoon Lee, Kelvin Xu, and Aviral Kumar. Scaling lilm test-time compute opti-
 396 mally can be more effective than scaling model parameters. *arXiv preprint arXiv:2408.03314*,
 397 2024.

398 [42] Robyn Speer, Joshua Chin, and Catherine Havasi. Conceptnet 5.5: An open multilingual graph
 399 of general knowledge. In *AAAI*, 2017.

400 [43] Alon Talmor, Jonathan Herzig, Nicholas Lourie, and Jonathan Berant. Commonsenseqa: A
 401 question answering challenge targeting commonsense knowledge. In *NAACL*, 2019.

402 [44] Xiaojuan Tang, Zilong Zheng, Jiaqi Li, Fanxu Meng, Song-Chun Zhu, Yitao Liang, and Muhan
 403 Zhang. Large language models are in-context semantic reasoners rather than symbolic reasoners.
 404 *arXiv preprint arXiv:2305.14825*, 2023.

405 [45] Gemini Team, Rohan Anil, Sebastian Borgeaud, Jean-Baptiste Alayrac, Jiahui Yu, Radu Soricut,
 406 Johan Schalkwyk, Andrew M Dai, Anja Hauth, Katie Millican, et al. Gemini: a family of highly
 407 capable multimodal models. *arXiv preprint arXiv:2312.11805*, 2023.

408 [46] Qwen Team. Qwq-32b: Embracing the power of reinforcement learning, March 2025. URL
 409 <https://qwenlm.github.io/blog/qwq-32b/>.

410 [47] Ian Tenney, Dipanjan Das, and Ellie Pavlick. Bert rediscovers the classical nlp pipeline. In
 411 *ACL*, 2019.

412 [48] Jean-Francois Ton, Muhammad Faaiz Taufiq, and Yang Liu. Understanding chain-of-thought in
 413 llms through information theory. *arXiv preprint arXiv:2411.11984*, 2024.

414 [49] Laurens van der Maaten and Geoffrey E. Hinton. Visualizing data using t-sne. *JMLR*, 2008.

415 [50] Boshi Wang, Sewon Min, Xiang Deng, Jiaming Shen, You Wu, Luke Zettlemoyer, and Huan
 416 Sun. Towards understanding chain-of-thought prompting: An empirical study of what matters.
 417 In *ACL*, 2023.

418 [51] Xinyi Wang, Alfonso Amayuelas, Kexun Zhang, Liangming Pan, Wenhui Chen, and
 419 William Yang Wang. Understanding the reasoning ability of language models from the perspec-
 420 tive of reasoning paths aggregation. In *ICML*, 2024.

421 [52] Xuezhi Wang, Jason Wei, Dale Schuurmans, Quoc V Le, Ed H. Chi, Sharan Narang, Aakanksha
 422 Chowdhery, and Denny Zhou. Self-consistency improves chain of thought reasoning in language
 423 models. In *ICLR*, 2023.

424 [53] Jason Wei, Xuezhi Wang, Dale Schuurmans, Maarten Bosma, Brian Ichter, Fei Xia, Ed H. Chi,
 425 Quoc V Le, and Denny Zhou. Chain of thought prompting elicits reasoning in large language
 426 models. In *NeurIPS*, 2022.

427 [54] Skyler Wu, Eric Meng Shen, Charumathi Badrinath, Jiaqi Ma, and Himabindu Lakkaraju.
 428 Analyzing chain-of-thought prompting in large language models via gradient-based feature
 429 attributions. *arXiv preprint arXiv:2307.13339*, 2023.

430 [55] Fengli Xu, Qianyue Hao, Zefang Zong, Jingwei Wang, Yunke Zhang, Jingyi Wang, Xiaochong
431 Lan, Jiahui Gong, Tianjian Ouyang, Fanjin Meng, et al. Towards large reasoning models: A
432 survey of reinforced reasoning with large language models. In *arXiv*, 2025.

433 [56] Shunyu Yao, Dian Yu, Jeffrey Zhao, Izhak Shafran, Thomas L. Griffiths, Yuan Cao, and
434 Karthik R Narasimhan. Tree of thoughts: Deliberate problem solving with large language
435 models. In *NeurIPS*, 2023.

436 [57] Shunyu Yao, Jeffrey Zhao, Dian Yu, Nan Du, Izhak Shafran, Karthik R Narasimhan, and Yuan
437 Cao. React: Synergizing reasoning and acting in language models. In *ICLR*, 2023.

438 [58] Yunzhi Yao, Ningyu Zhang, Zekun Xi, Mengru Wang, Ziwen Xu, Shumin Deng, and Huajun
439 Chen. Knowledge circuits in pretrained transformers. In *NeurIPS*, 2024.

440 [59] Xi Ye, Srinivasan Iyer, Asli Celikyilmaz, Ves Stoyanov, Greg Durrett, and Ramakanth Pasunuru.
441 Complementary explanations for effective in-context learning. *arXiv preprint arXiv:2211.13892*,
442 2022.

443 [60] Eric Zelikman, Yuhuai Wu, Jesse Mu, and Noah Goodman. Star: Bootstrapping reasoning with
444 reasoning. In *NeurIPS*, 2022.

445 [61] Dan Zhang, Sining Zhoubian, Ziniu Hu, Yisong Yue, Yuxiao Dong, and Jie Tang. Rest-mcts*:
446 Llm self-training via process reward guided tree search. In *NeurIPS*, 2024.

447 [62] Denny Zhou, Nathanael Schärli, Le Hou, Jason Wei, Nathan Scales, Xuezhi Wang, Dale
448 Schuurmans, Claire Cui, Olivier Bousquet, Quoc V Le, and Ed H. Chi. Least-to-most prompting
449 enables complex reasoning in large language models. In *ICLR*, 2023.

450 [63] Zhaocheng Zhu, Yuan Xue, Xinyun Chen, Denny Zhou, Jian Tang, Dale Schuurmans, and
451 Hanjun Dai. Large language models can learn rules. *arXiv preprint arXiv:2310.07064*, 2023.

452 **Appendix**

453	A Impact Statement	14
454	B Further Discussions	14
455	B.1 Challenges in Analyzing LLM’s Reasoning Automatically	14
456	B.2 A Comparison Between Landscape Visualization and Textual Analysis	15
457	B.3 A Comparison Between Lightweight Verifier and Reward-guided Algorithms . . .	15
458	C Experiment Settings	16
459	C.1 Settings	16
460	C.2 Datasets	16
461	C.3 Decoding Algorithms	17
462	D Supplementary Results and Analysis	17
463	D.1 Statistical Verification of the Observations	17
464	D.2 Robustness of Sentence Tokenization	18
465	D.3 Absolute Performance of the Verifier	18
466	D.4 Variants of Verifier	18
467	D.5 Further Discussion on the StrategyQA	19
468	E Visualizations	19

469 **A Impact Statement**

470 Our work presents a tool for visualizing and understanding reasoning steps in large language models.
471 We foresee that our work will introduce more interpretability and transparency into the development
472 and deployment of LLMs, advancing us toward more trustworthy machine learning. However, we
473 must acknowledge that malicious activities can also be augmented by our tool. For example, attackers
474 may use this tool to find prompts that bypass the alignment safeguards in LLMs. We believe such
475 risks will be mitigated if this tool is widely adopted by safety researchers. Overall, the positive
476 societal consequences of our work outweigh the negative ones, which stem primarily from misuse.

477 **B Further Discussions**

478 In this section, we further discuss the challenges in developing the system for analyzing LLMs’
479 reasoning (Appendix B.1), followed by comparing the proposed landscape visualization technique
480 with the textual analysis methodology (Appendix B.2). In addition, we compare the lightweight
481 verifier to conventional reward-guided algorithms (Appendix B.3).

482 **B.1 Challenges in Analyzing LLM’s Reasoning Automatically**

483 Currently, the fundamental mechanisms behind both successful and unsuccessful reasoning attempts
484 in LLMs remain inadequately understood. Traditional performance metrics, such as accuracy, provide
485 insufficient insights into model behavior. While human evaluation has been employed to assess
486 the quality of sequential thoughts (e.g., logical correctness and coherence), such approaches are
487 resource-intensive and difficult to scale. We identify three challenges in developing *automated*
488 *analysis systems* for LLMs’ reasoning:

489 *Challenge 1: Bridging the token-thought gap.* Current explanatory tools, including attention maps [7,
490 24], probing [2, 47, 17], and circuits [12, 58], primarily operate at the token-level explanation. While

491 these approaches offer valuable insights into model inference, they struggle to capture the emergence
492 of higher-level reasoning patterns from lower-level token interactions. Additionally, the discrete
493 nature of natural language thoughts poses challenges for traditional statistical analysis tools designed
494 for continuous spaces. Understanding how thought-level patterns contribute to complex reasoning
495 capabilities requires new analytical frameworks that can bridge this conceptual gap.

496 *Challenge 2: Analyzing without training data access.* Existing investigations into LM reasoning
497 have predominantly focused on correlating test questions with training data [18, 51]. This approach
498 becomes particularly infeasible given the reality of modern LLMs: many models are closed-source,
499 while some offer only model weights. Therefore, a desired analysis framework should operate across
500 varying levels of model accessibility.

501 *Challenge 3: Measuring reasoning quality.* Beyond simple performance metrics, we need new ways
502 to evaluate the quality and reliability of model reasoning. This includes developing techniques to
503 understand reasoning paths, creating intermediate representations that capture both token-level and
504 thought-level patterns, and designing metrics that can assess the logical coherence and validity of
505 reasoning steps.

506 Consequently, we propose that a viable analysis of reasoning behavior should satisfy multiple criteria:
507 it should operate in a post-hoc manner with varying levels of model access, bridge the gap between
508 token-level and thought-level analysis, and provide meaningful metrics for evaluating reasoning
509 quality. Given the absence of tools meeting these requirements, we identify the need for a new
510 analytical framework that can address these challenges while providing useful insights for improving
511 model reasoning capabilities.

512 **B.2 A Comparison Between Landscape Visualization and Textual Analysis**

513 Notably, for the language model, one could manually examine the responses of individual samples,
514 as their responses are interpretable by humans. However, this approach has two major limitations:

515 *Limitation 1: Lack of Scalability.* Analyzing individual samples is time-consuming and labor-
516 intensive. In general, text-based analysis requires human evaluators to carefully read long reasoning
517 chains word by word. For example, if it takes 30 seconds to understand a single sample, reviewing
518 100 samples would require around 50 minutes of focused human effort. This burden grows quickly,
519 especially as researchers often repeat this process many times while developing models and methods.
520 In practice, researchers need quick, easily interpretable feedback like accuracy when experimenting
521 with changes to models and methods.

522 *Limitation 2: Lack of Aggregation.* It is difficult to aggregate insights across multiple samples to
523 understand model behavior at the dataset level. Summarizing model behavior across multiple samples
524 presents another challenge. Suppose one researcher has 100 reasoning chains, it is hard for him/her
525 to reliably synthesize the model’s overall behavior. Different researchers may arrive at different,
526 subjective summaries, which hinders consistency and interpretability.

527 By contrast, our visualization method provides a more objective and automatic way to analyze a
528 model, making it much easier for researchers to analyze the model’s reasoning behavior. Similar
529 to the t-SNE [49], the visualization enables a more comprehensive analysis of multiple reasoning
530 samples instead of only one sample. The visualization uniquely combines human-readable paths with
531 quantitative, scalable metrics for reasoning process analysis, enabling both model comparisons and
532 mechanistic insights beyond manual text inspection.

533 Notably, the landscape provides unique insights into LLM reasoning that text analysis alone cannot
534 capture. This power source bridges the gap between localized text understanding and global reasoning
535 behavior. Our analysis in Sec. 3 reveals insights that are not revealed by previous text-based analysis.
536 These insights include structural patterns across many reasoning paths, a strong correlation between
537 early consistency and accuracy, and model-level differences where larger models explore more
538 broadly than smaller ones.

539 **B.3 A Comparison Between Lightweight Verifier and Reward-guided Algorithms**

540 It is worth noting to mention that our goal is not to build a sophisticated verifier, but rather to
541 demonstrate how the feature vectors from the landscape visualization can be effectively used.

542 In general, reward-guided algorithms are more computationally efficient than the path landscape.
543 Specifically, for a reasoning path with n thoughts and c answer choices, constructing the landscape
544 requires $n \times c$ forward passes through the reasoning model. In contrast, a reward-guided approach
545 typically makes a single call to a reward model that evaluates the entire reasoning chain at once.
546 Meanwhile, it's important to consider the overhead involved in training the reward models in reward-
547 guided algorithms. Notably, for Process-Reward Models (PRMs) [30, 55], collecting high-quality
548 training data often requires detailed, fine-grained annotations of reasoning steps, which can be costly
549 and time-consuming. Moreover, training a reward model (often itself a LLM) incurs significant
550 computational expense. In contrast, our lightweight verifier is much more efficient to train, as it
551 requires no human annotations and uses easily obtainable data.

552 C Experiment Settings

553 C.1 Settings

554 Visualizing the landscape of thoughts fundamentally relies on the decoding probability of LLMs. To
555 this end, we adopted four open-source models with varying parameter sizes, namely Llama-3.2-1B,
556 Llama-3.2-3B, Llama-3.1-8B, and Llama-3.1-70B. We repeatedly sample 10 times from the
557 target LLM using the same reasoning strategy as self-consistency [52].

558 For visualization purposes, we randomly sample 50 questions from the testing split of each dataset
559 and generate reasoning paths with the setup described above. For simplicity, we compute distances
560 only between each state and all candidate answers. To visualize multiple samples in a shared space,
561 we always place the distance to the correct answer as the first element of each feature vector. This
562 alignment allows joint analysis across samples, as introduced in the paragraph below Equation 4. We
563 then aggregate feature vectors from all samples into a feature matrix (Equation 2), which is passed to
564 t-SNE to compute the pairwise distance between any two states and then outputs the 2D coordinate
565 of each state.

566 For training the lightweight verifier, we randomly sample 20 questions from the training split of
567 each dataset to obtain the feature matrix S . We extract these features using three model scales:
568 Llama-3.2-3B, Llama-3.1-8B, and Llama-3.1-70B. Despite the relatively small training set,
569 it proves sufficient for our lightweight verifier, which we subsequently evaluate on the data for
570 visualization in Sec. 3.

571 C.2 Datasets

572 **AQuA** [28]. This dataset develops to challenge language models' quantitative reasoning capabilities.
573 The AQuA presents complex algebraic word problems in a multiple-choice format, where only one is
574 correct. Each problem requires numerical computation, deep linguistic understanding, and logical
575 inference. It provides a nuanced assessment of a model's ability to translate textual information into
576 algebraic reasoning.

577 **MMLU** [16]. Spanning 57 distinct academic and professional domains, MMLU provides a rigorous
578 test of language models' capabilities across humanities, social sciences, hard sciences, and technical
579 disciplines.

580 **StrategyQA** [13]. This dataset is designed to evaluate implicit reasoning and multi-hop question
581 answering. The dataset is characterized by yes/no questions that demand implicit reasoning strategies.
582 Unlike straightforward factual queries, these questions require models to construct elaborate reasoning
583 paths, showing hidden logical connections.

584 **CommonsenseQA** [43]. This dataset assesses commonsense reasoning through multi-choice ques-
585 tions derived from the ConceptNet knowledge graph [42]. The dataset aims to test a model's
586 understanding of commonsense concepts and ability to make logical inferences. However, the ques-
587 tions often require the model to incorporate external knowledge to select the correct answer from
588 plausible distractors.

589 Note that AQuA, MMLU, and StrategyQA all demand exploratory traversal of intermediate reasoning
590 states, resulting in diverse but structured landscapes. CommonsenseQA, conversely, represents a
591 distinct domain where answers depend on static knowledge rather than emergent reasoning pathways.

Table 1: Statistical verification of the observations in Sec. 3.

(a) Verifying Obs. 3.1		(b) Verifying Obs. 3.2 and 3.6		(c) Verifying Obs. 3.4			
Correct	Incorrect	Speed	Accuracy	AQuA	MMLU	StrategyQA	Common SenseQA
CoT	1.026	0.975	0.322	84.4%			
L2M	1.026	0.989	0.224	82.2%			
ToT	1.004	0.987	0.205	81.6%			
MCTS	1.002	0.985	0.198	75.8%			

592 C.3 Decoding Algorithms

593 **Chain of Thought (CoT)** [53]. CoT elicits the LLM’s reasoning capabilities by incorporating
 594 few-shot examples that demonstrate explicit reasoning steps. It provides the model with exemplar
 595 reasoning traces to guide its problem-solving process.

596 **Zero-shot CoT** [25]. The core idea of this prompt strategy lies in adding simple instructions, e.g.,
 597 “Let’s think step by step.” to the prompt, enabling models to generate reasoning traces without
 598 assigned task-specific examples.

599 **Least-to-Most (LtM)** [62]. LtM is an innovative reasoning approach that systematically breaks down
 600 complex problems into progressively simpler subproblems. This approach mirrors human cognitive
 601 problem-solving strategies, where individuals naturally break down complex tasks into smaller, more
 602 comprehensible parts.

603 **Tree-of-Thought (ToT)** [56]. ToT expanded this concept by creating a more sophisticated, multi-
 604 branching reasoning framework. While CoT follows a linear path of reasoning, ToT introduces a
 605 more dynamic exploration, allowing models to generate multiple reasoning paths simultaneously,
 606 evaluate them, and strategically prune less promising trajectories.

607 **Monte Carlo tree search (MCTS)** [61]. MCTS is a powerful computational algorithm originally
 608 developed for game-playing strategies, particularly in complex decision-making environments like
 609 chess and Go. The method uses probabilistic sampling and tree exploration to systematically navigate
 610 potential solution spaces, balancing exploring new possibilities with exploiting promising paths. We
 611 adopt the task-agnostic node expansion and evaluation prompt from ReST-MCTS [61] to conduct our
 612 experiment across different tasks.

613 **Reproduction.** The source code is provided in the anonymous repository: <https://anonymous.4open.science/r/landscape-of-thoughts-submission-code-3803/>.

615 D Supplementary Results and Analysis

616 D.1 Statistical Verification of the Observations

617 In this part, we conduct extra experiments and statistically verify Obs. 3.1, 3.2, 3.4, and 3.6, while
 618 the other Obs. 3.3, 3.5, and 3.7 have been quantitatively verified by the metrics in Sec. 2.3.

619 To verify Obs. 3.1, we calculate the convergence coefficient (e^β) by fitting a log-linear regression
 620 model to the sequence of distances d_i between each state and the final answer as $\log(d_i) \approx \alpha + \beta i$,
 621 where α is the intercept term; β is the slope coefficient that quantifies convergence behavior; i
 622 represents the position index in the reasoning chain. Lower values of e^β indicate faster convergence.
 623 For Obs. 3.2 and 3.6, we measure the speed of a reasoning path moving from start to end as
 624 speed = $\frac{\|\bar{s}_n - \bar{s}_0\|}{\sum_{j=1}^n \|\bar{s}_j - \bar{s}_{j-1}\|} \in [0, 1]$, where \bar{s}_i represents the 2D coordinate of the state i . Whereas
 625 Obs. 3.4, we compute pairwise histogram intersection scores of the density distributions. Lower
 626 scores indicate greater dissimilarity between landscapes.

627 Notably, for Tab. 1(a), we found that correct paths consistently show slight divergence, while incorrect
 628 paths show more convergence (p-value = 0.008), thus verifying Obs. 3.1. As shown in Tab. 1(b),
 629 speed and accuracy correlate strongly (p-value = 9.421e-11), thus verifying Obs. 3.2. This is also
 630 applicable for verifying Obs. 3.6. Tab. 1(c) shows that lower scores indicate greater dissimilarity

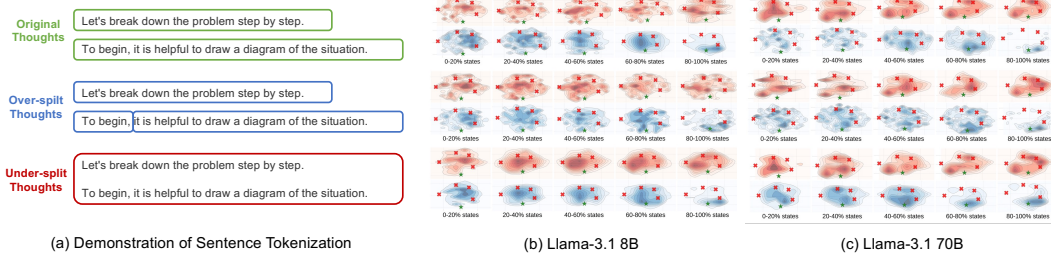


Figure 8: Demonstration of sentence tokenization methods for thoughts splitting.

Table 2: Absolute accuracy with the verifier, compared to performance in Fig. 5 (without the verifier).

(a) Across datasets				(b) Across models				
	AQuA	MMLU	StrategyQA	Common SenseQA	1B	3B	8B	70B
AQuA	63.0 (+0.7)	62.3 (+0.0)	62.3 (+0.0)	64.0 (+1.7)	1B	26.0 (+0.5)	27.5 (+2.0)	27.5 (+2.0)
MMLU	53.0 (+0.0)	53.0 (+0.0)	53.0 (+0.0)	53.0 (+0.0)	3B	45.5 (+0.0)	48.0 (+2.5)	51.0 (+5.5)
StrategyQA	41.5 (+4.5)	40.5 (+3.5)	43.0 (+6.0)	37.0 (+0.0)	8B	60.0 (+0.0)	60.0 (+0.0)	60.0 (+0.0)
Common SenseQA	54.0 (+1.0)	53.0 (+0.0)	53.0 (+0.0)	54.0 (+1.0)	70B	74.0 (+2.0)	73.0 (+1.0)	72.5 (+0.5)

631 between landscapes, which verifies Obs. 3.4, i.e., AQuA, MMLU, and StrategyQA are more similar,
632 while CommonSenseQA exhibits distinct patterns.

633 D.2 Robustness of Sentence Tokenization

634 To evaluate the robustness of the landscape to the split thoughts’ information volume, *i.e.*, the
635 granularity of the sentence tokenization, we conduct the controlled experiment by considering two
636 imperfect cases in thought split, namely over-split thoughts and under-split thoughts.

637 Specifically, shown as Fig. 8 (a), compared to the original thoughts split that transform sentences to
638 thoughts based on the period, over-split thoughts jointly consider the comma, resulting in additional
639 splits. For the under-split, two adjacent thoughts are merged into one thought. We then visualize the
640 imperfect thought splits using CoT on AQuA following the setting in Fig. 2(a) and Fig. 4(c),

641 Shown in Fig. 8 (b) and (c), the landscapes are robust to the split thoughts’ information volume,
642 which are stable and consistent with our observations. Notably, for over-split thoughts, the states
643 are more visually diverse but eventually converge to the answers. Whereas under-split thoughts, the
644 states show a more compact pattern and exhibit a clear convergence trend toward the answer.

645 D.3 Absolute Performance of the Verifier

646 In this part, we provide the absolute performance of the experiment conducted in Fig. 7. Shown as
647 Tab. 2, the results demonstrate that our approach consistently provides improvements across different
648 domains and models.

649 D.4 Variants of Verifier

650 In this part, we extend it into a process verifier and validate its effectiveness through additional
651 experiments. Our lightweight verifier functions as an outcome reward model (ORM), assessing the
652 correctness of an entire reasoning path. Specifically, the process verifier predicts the accuracy of
653 each reasoning state using features from the current and all previous thoughts. State accuracy reflects
654 whether the current state is closer to the correct answer (measured by perplexity) than other answers.
655 We then aggregate these predictions across the chain to estimate overall accuracy.

656 Empirically, we collect the state-wise data by comparing the state features and the correct answers,
657 and train the process verifier. Note, we do not need to manually annotate the step-wise rewards
658 to train conventional PRMs. Results in Tab. 3 show that this process verifier is comparable to the
659 outcome verifier.

Table 3: Performance comparison of reasoning methods across model scales on the AQuA dataset, with and without verifiers.

Model	Method	Without Verifier	With Outcome Verifier	With Process Verifier
Llama-3.2-1B	CoT	0.26	0.28	0.26
	L2M	0.22	0.24	0.29
	ToT	0.35	0.38	0.35
	MCTS	0.29	0.32	0.31
Llama-3.2-3B	CoT	0.46	0.51	0.46
	L2M	0.29	0.31	0.31
	ToT	0.33	0.35	0.33
	MCTS	0.35	0.36	0.35
Llama-3.1-8B	CoT	0.60	0.63	0.60
	L2M	0.58	0.62	0.58
	ToT	0.50	0.53	0.50
	MCTS	0.50	0.51	0.50
Llama-3.1-70B	CoT	0.72	0.73	0.73
	L2M	0.72	0.72	0.73
	ToT	0.74	0.74	0.74
	MCTS	0.72	0.73	0.72

660 D.5 Further Discussion on the StrategyQA

661 The abnormal reasoning behavior, where states cluster on anchors that differ from their final answer
 662 in Fig. 3(c), is not due to our visualization method but to the unstable reasoning process in the Llama-
 663 3.1-70B using CoT on StrategyQA. This model struggles to reliably represent its self-generated
 664 intermediate thoughts, presenting consistency between intermediate thoughts and final predictions,
 665 thus leading to the abnormal patterns observed.

666 Specifically, the consistency of incorrect paths declines steadily. This highlights the model’s unstable
 667 reasoning, as it fails to maintain coherent reasoning even when approaching the final answer. In
 668 addition, the landscape exhibits the highest perplexity compared to other models, indicating low
 669 confidence in its generated thoughts, which undermines the reliability of the estimated feature matrix
 670 used in our visualization.

671 Further, we provide landscape visualizations for the same dataset using other models and methods in
 672 Fig. 9 to Fig. 12. These landscapes do not exhibit the same abnormal density patterns, reinforcing that
 673 the issue is specific to Llama-3.1-70B’s reasoning instability rather than a flaw in our visualization
 674 framework.

675 E Visualizations

676 In this part, we provide the full visualization of the verifier performance and landscapes.

677 In Fig. 13 to Fig. 16, we visualize the average voting accuracy (%) of different LLMs reasoning
 678 with and without verification on various datasets and methods. In Fig. 17 to Fig. 20, we display the
 679 landscape of different models on various datasets using four methods. We also provide case studies
 680 by visualizing the landscape with corresponding states in Fig 21 to Fig. 24.

681 In addition, we provide the landscape of thoughts on the latest reasoning model. Specifically, we
 682 conduct experiments on the QwQ-32 B [46] and DeepSeek-R1-Distill model [14] (Llama-70 B and
 683 Qwen-1.5 B). As shown in Fig. 25 to Fig. 27, the landscape of the reasoning model also aligns with
 684 the observation drawn from the general-purpose model, but exhibits more complex reasoning patterns,
 685 such as self-evaluation and back-tracking.

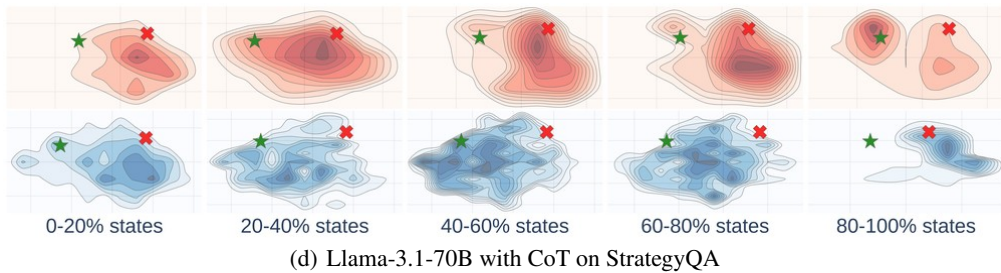
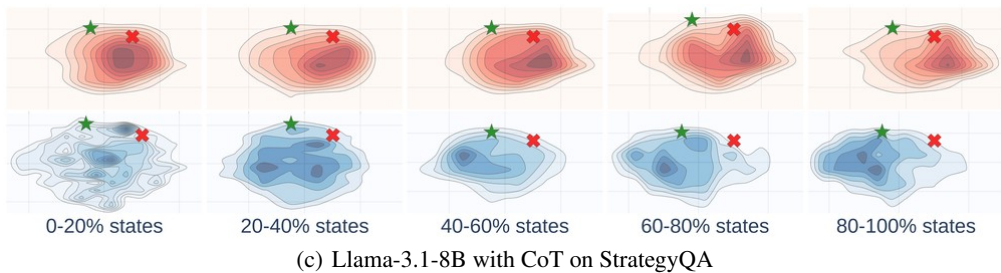
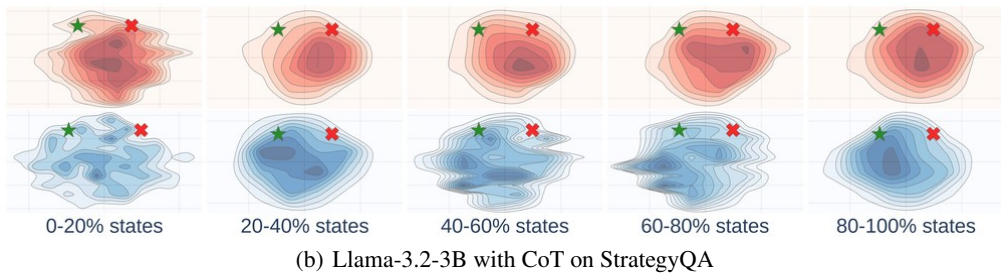
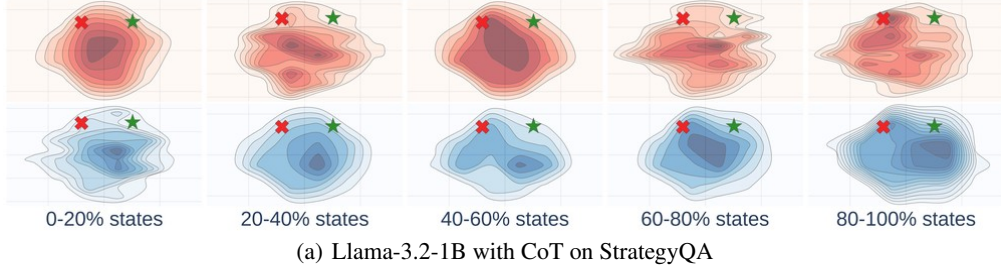


Figure 9: The landscapes of the model across scales (using CoT on the StrategyQA dataset).

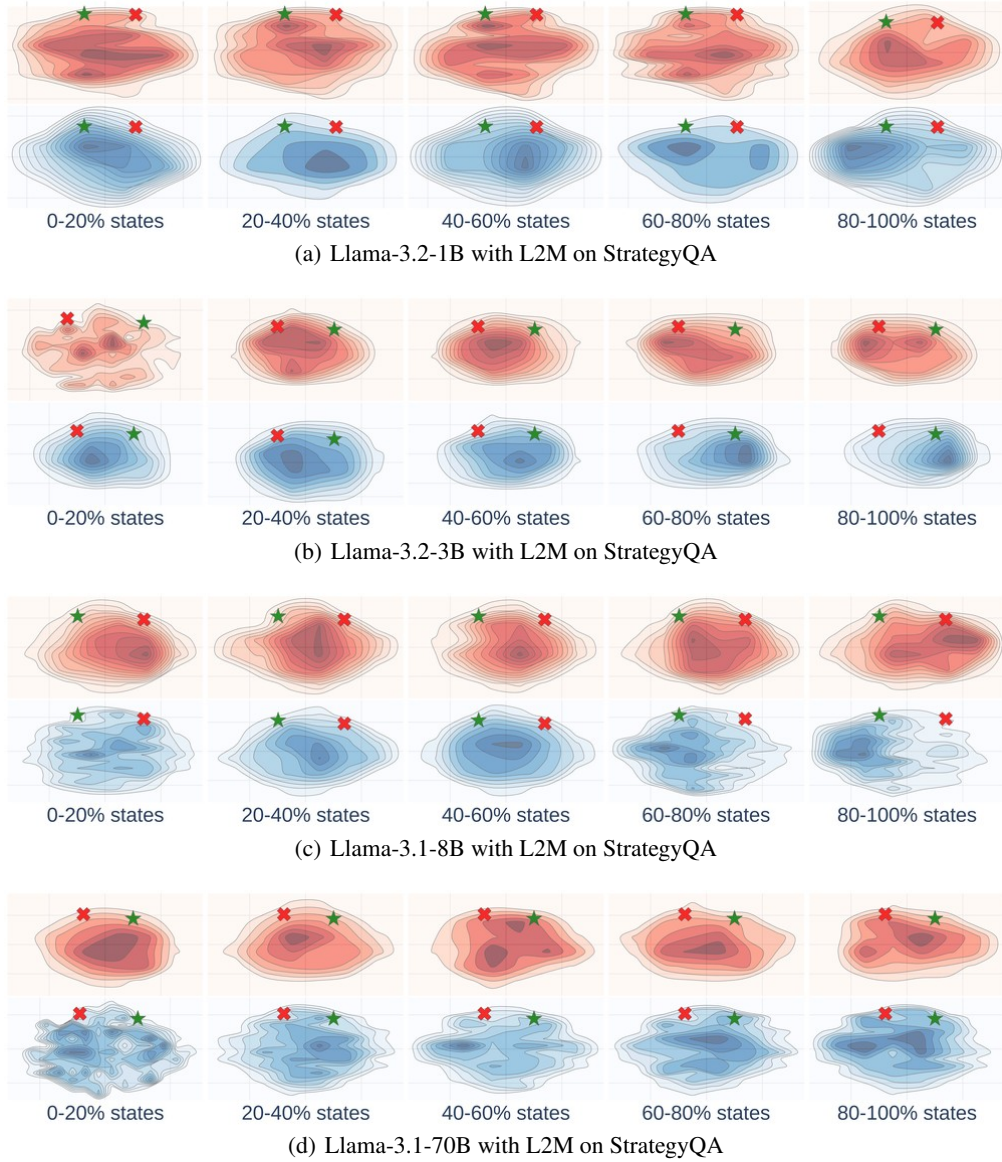


Figure 10: The landscapes of the model across scales (using L2M on the StrategyQA dataset).

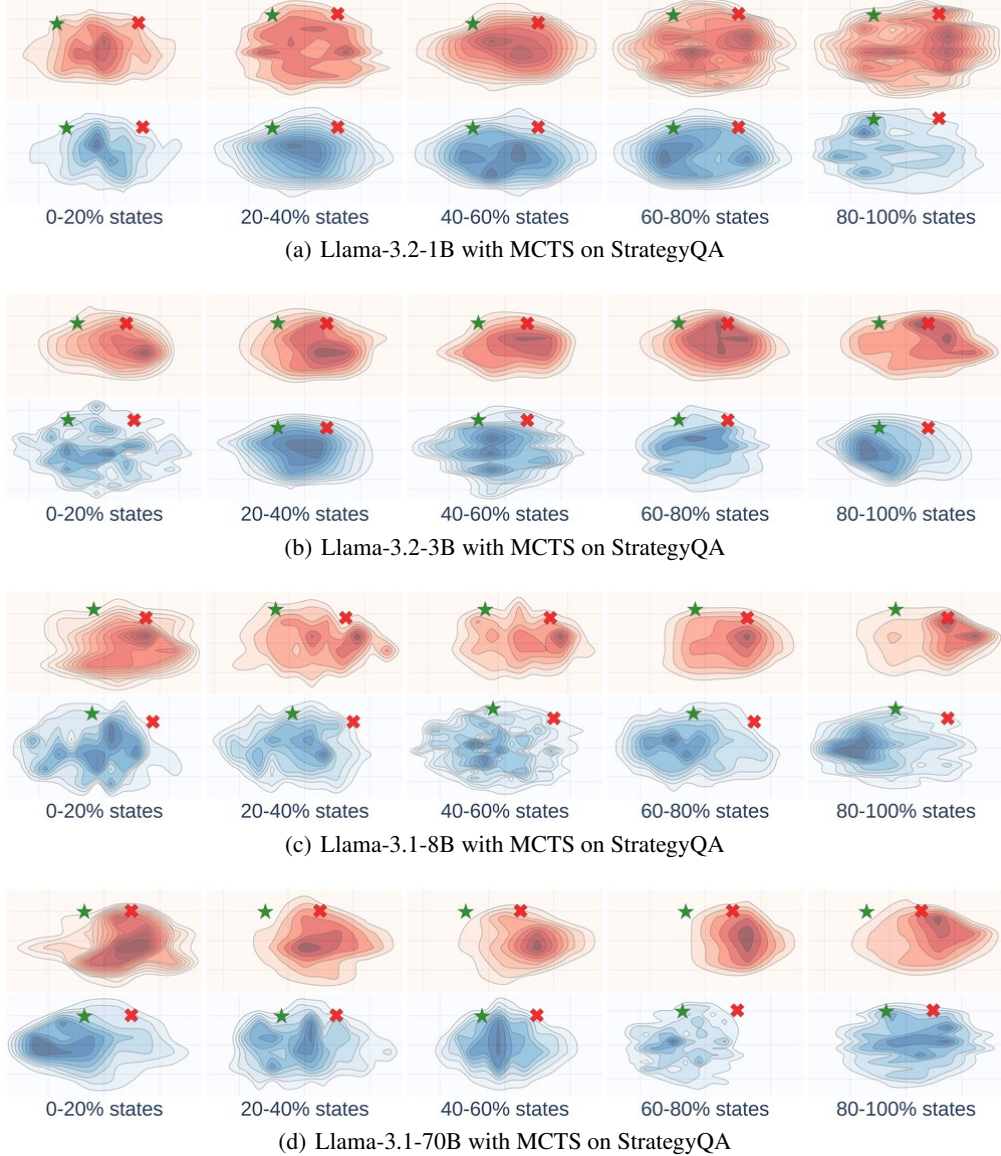


Figure 11: The landscapes of the model across scales (using MCTS on the StrategyQA dataset).

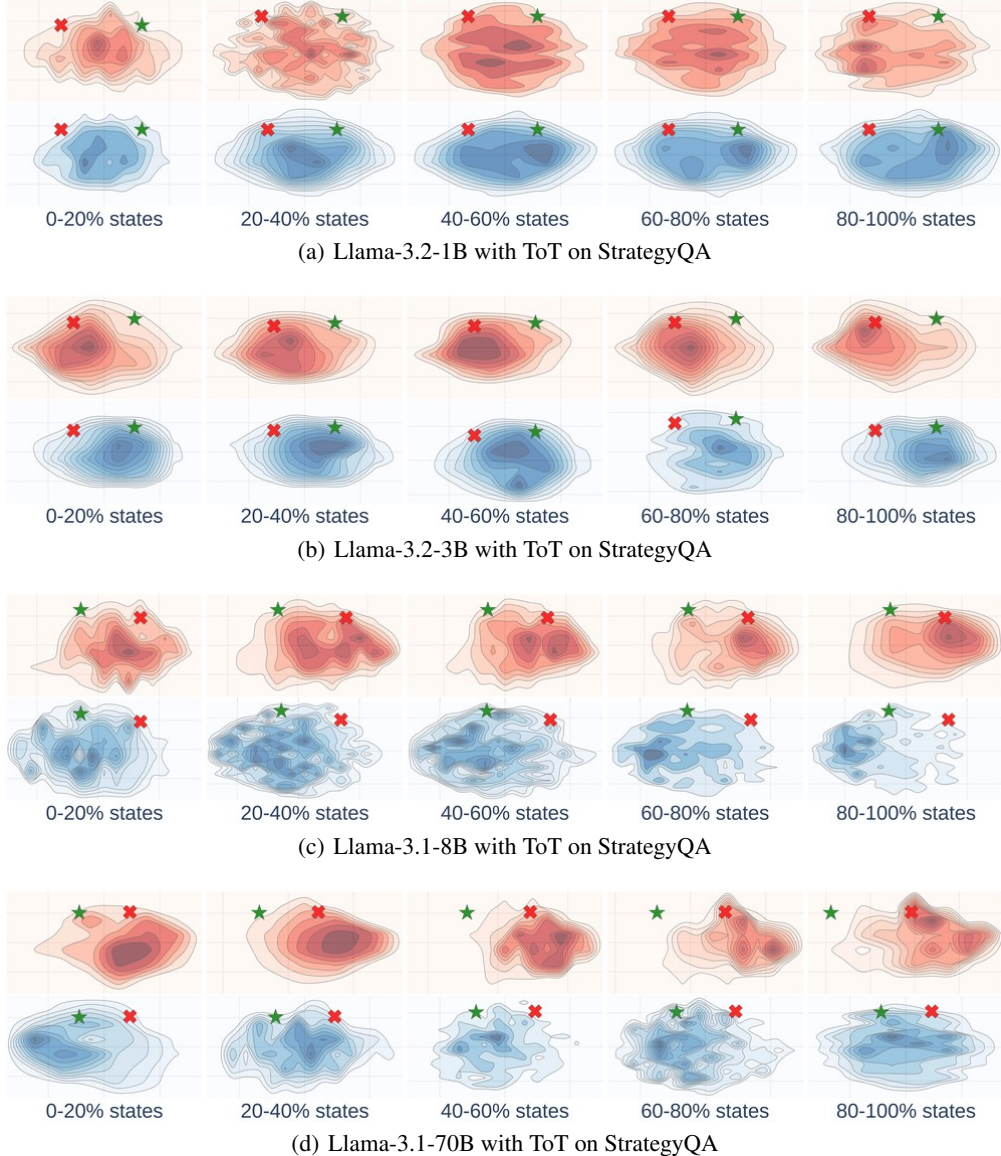


Figure 12: The landscapes of the model across scales (using ToT on the StrategyQA dataset).

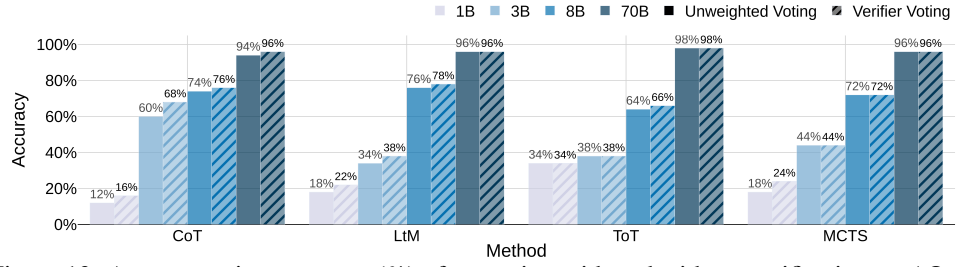


Figure 13: Average voting accuracy (%) of reasoning with and without verification on AQuA.

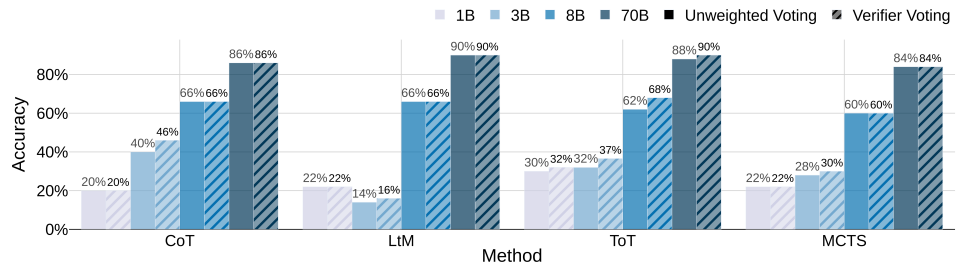


Figure 14: Average voting accuracy (%) of reasoning with and without verification on MMLU.

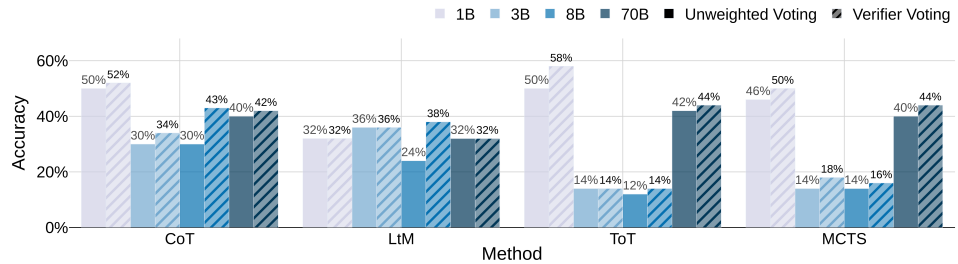


Figure 15: Average voting accuracy (%) of reasoning with and without verification on StrategyQA.

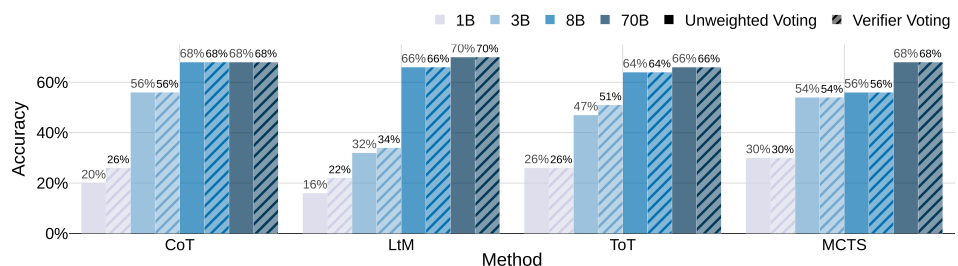


Figure 16: Average voting accuracy (%) of reasoning with and without verification on CommonsenseQA.

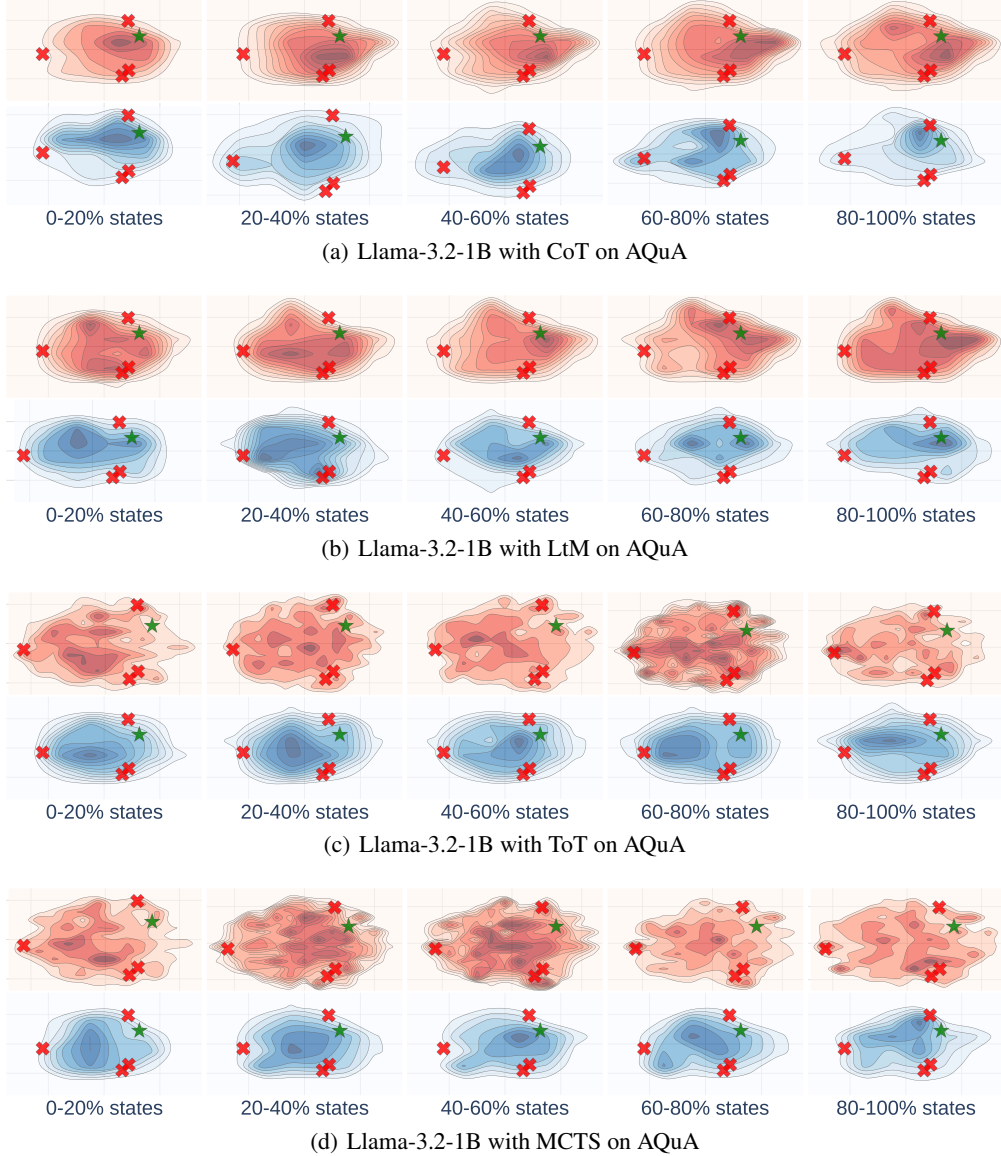


Figure 17: The landscapes of various reasoning methods (using Llama-3.2-1B on the AQuA dataset).

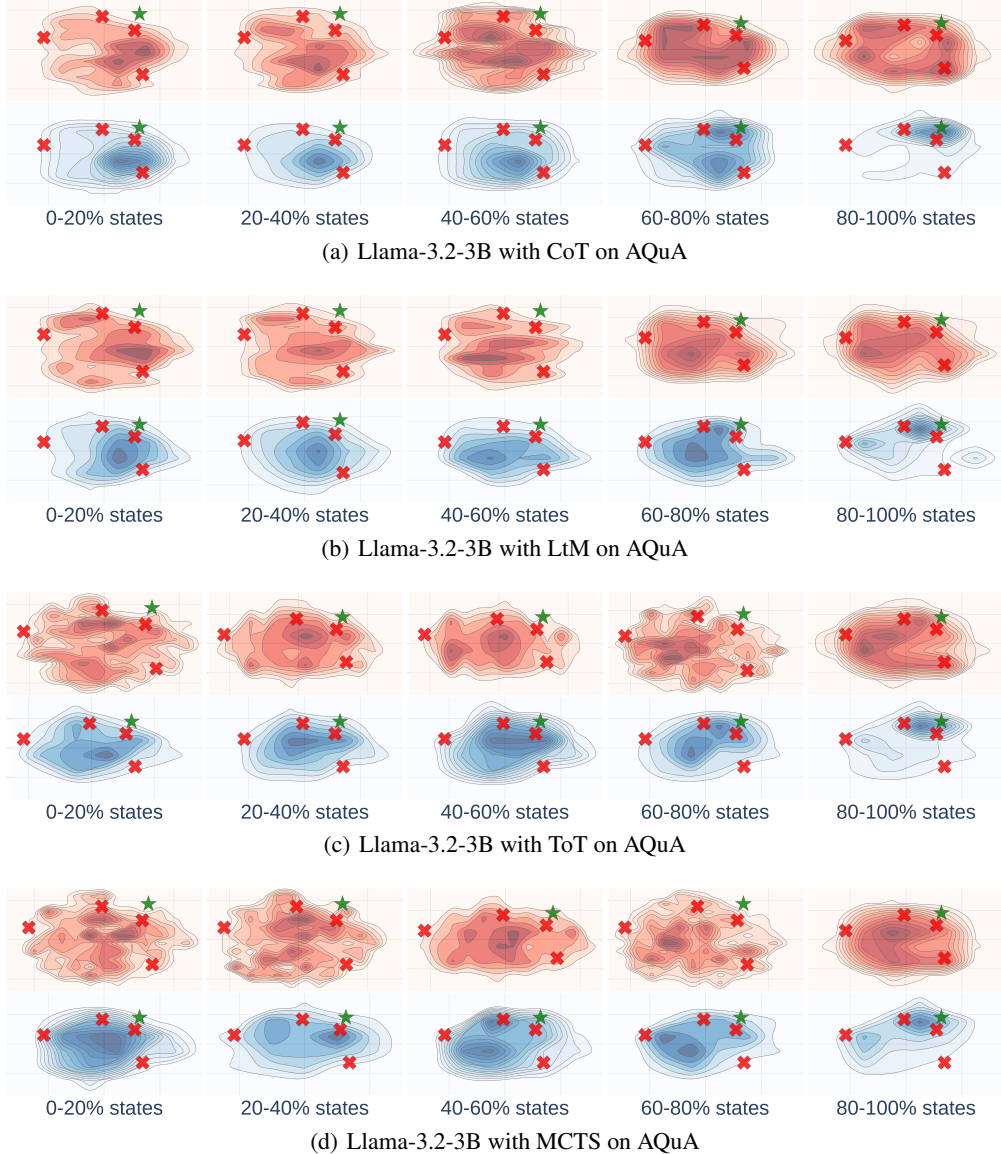


Figure 18: The landscapes of various reasoning methods (using Llama-3.2-3B on the AQuA dataset).

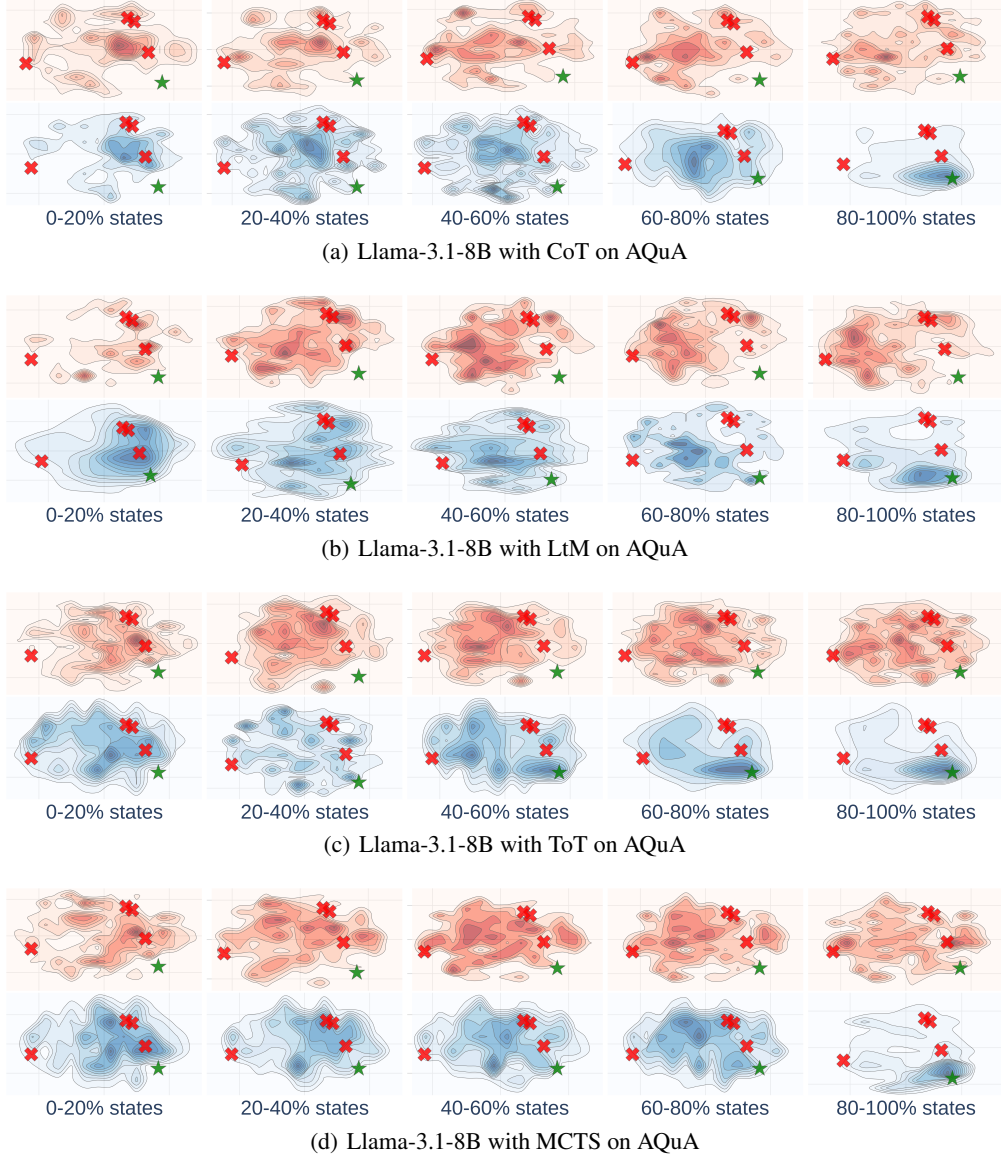


Figure 19: The landscapes of various reasoning methods (using Llama-3.1-8B on the AQuA dataset).

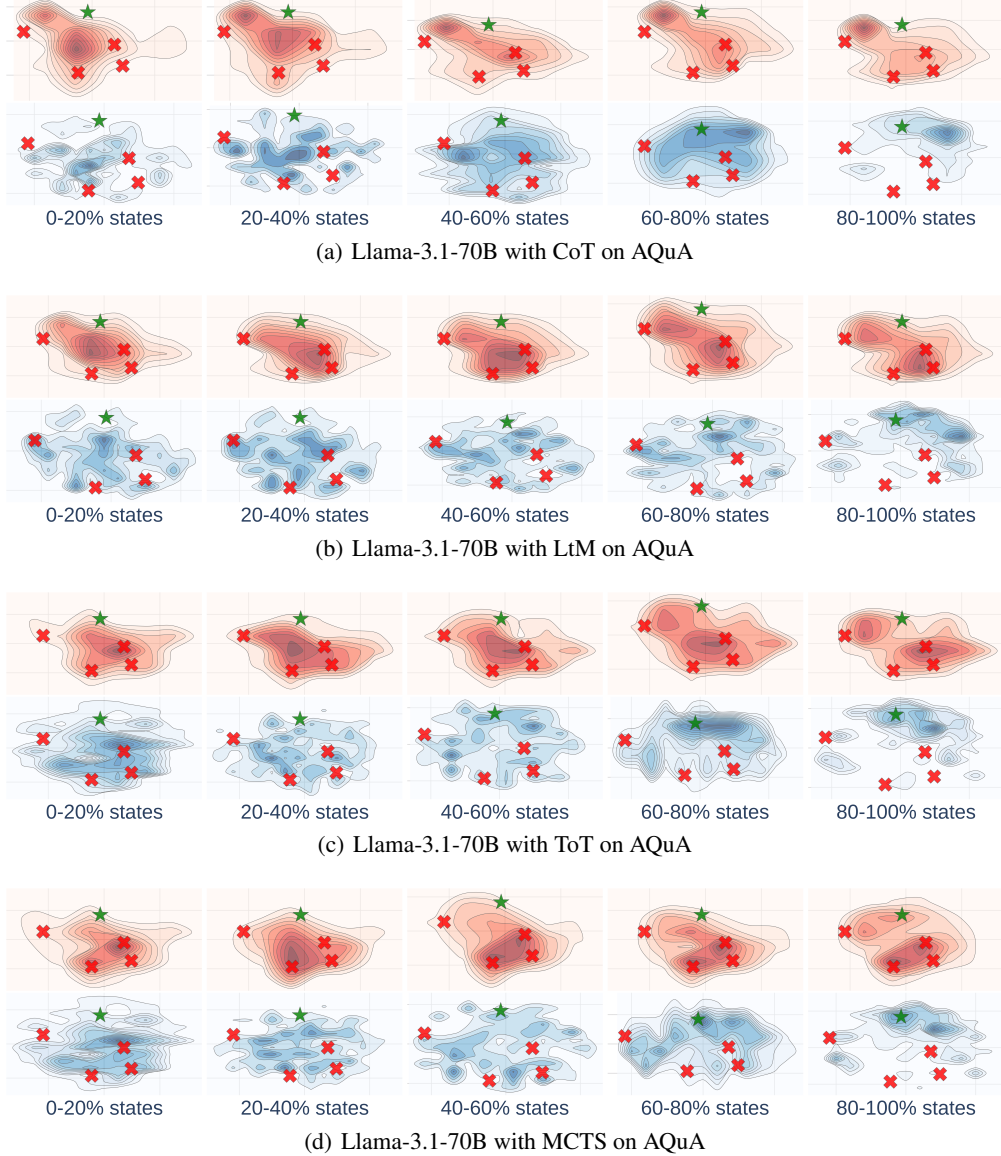


Figure 20: The landscapes of various reasoning methods (using Llama-3.1-70B on the AQuA dataset).

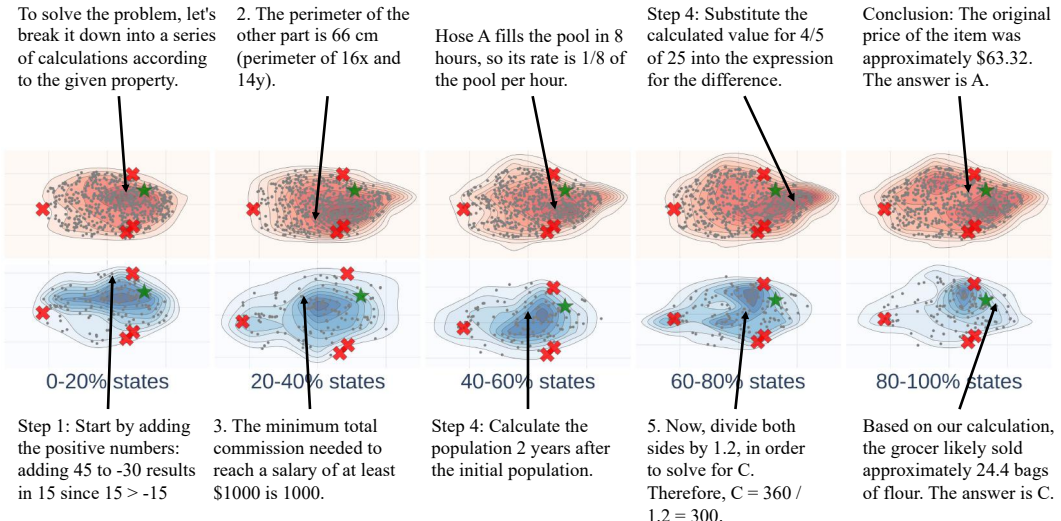


Figure 21: Case Study: Landscape of thoughts of Llama-3.2-1B on AQuA using CoT.

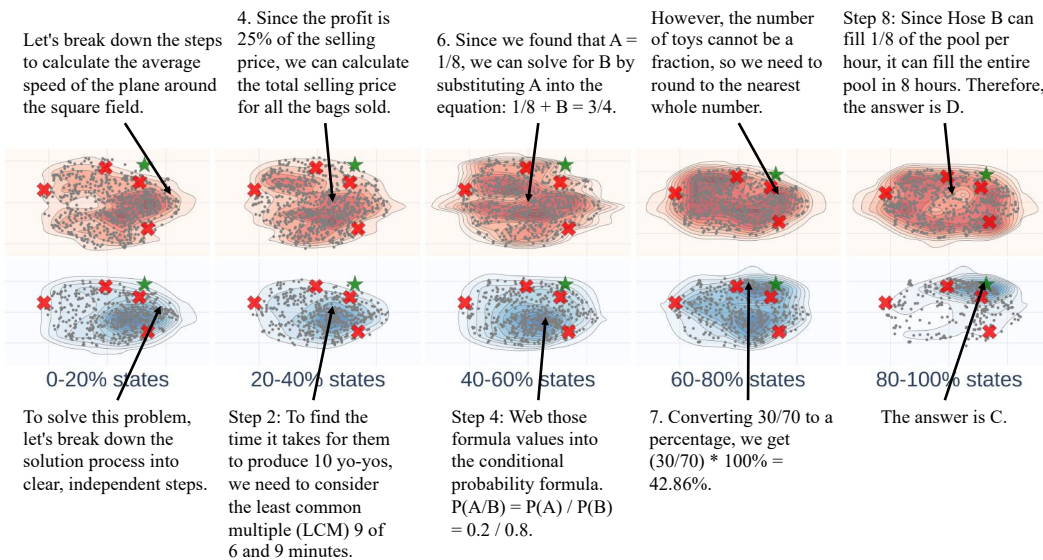


Figure 22: Case Study: Landscape of thoughts of Llama-3.2-3B on AQuA using CoT.

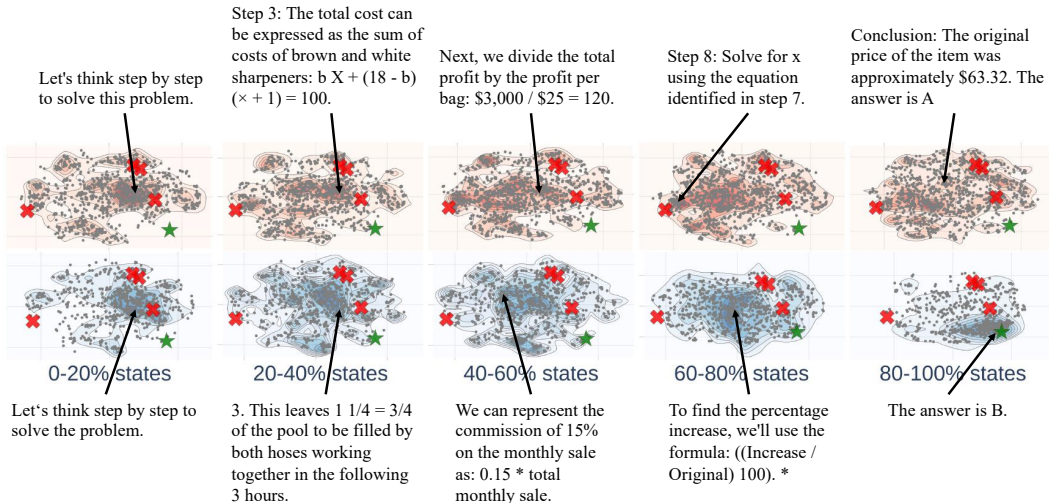


Figure 23: Case Study: Landscape of thoughts of Llama-3.1-8B on AQuA using CoT.

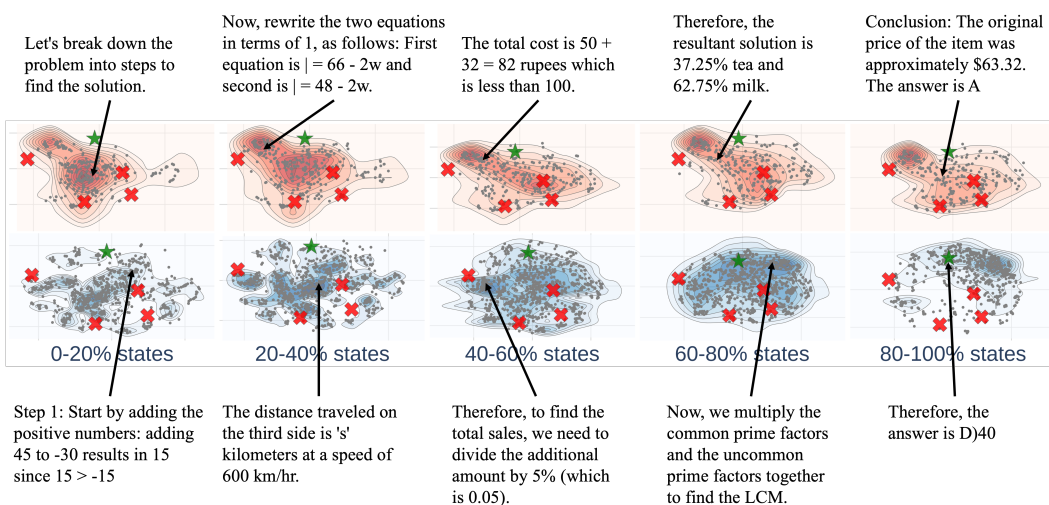


Figure 24: Case Study: Landscape of thoughts of Llama-3.1-70B on AQuA using CoT.

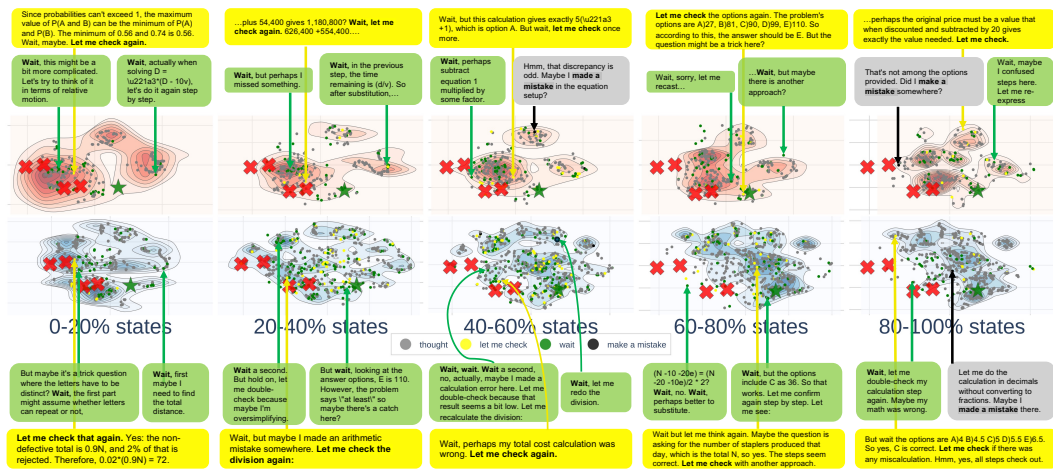


Figure 25: Landscape of QwQ-32B using CoT on AQuA.

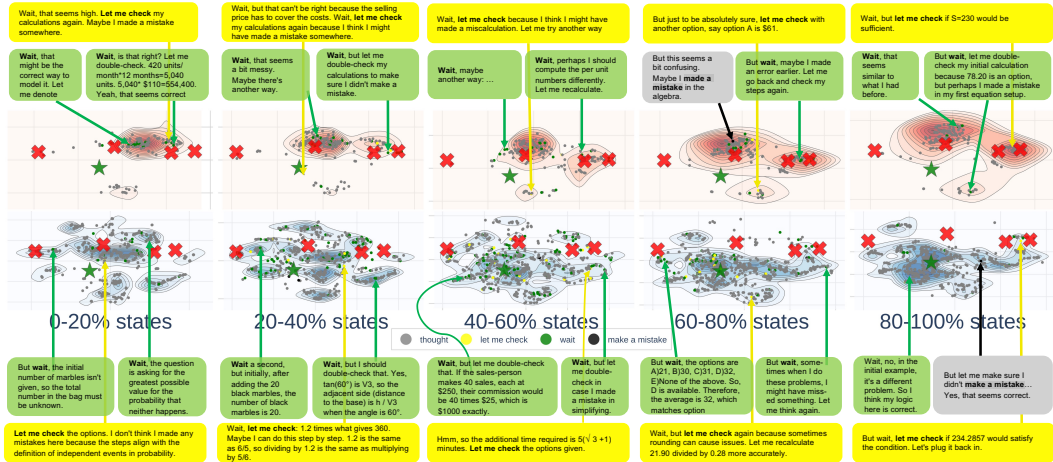


Figure 26: Landscape of DeepSeek-R1-Distill-Llama-70B using CoT on AQuA.

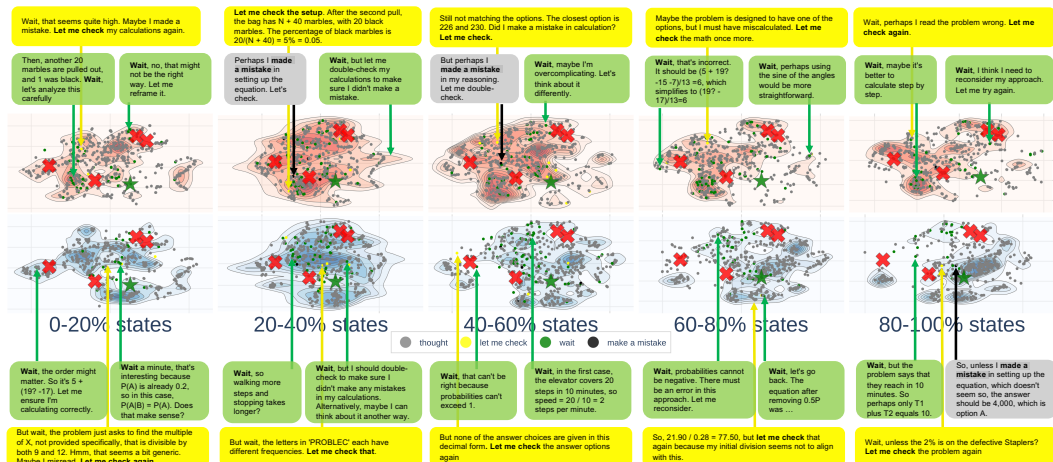


Figure 27: Landscape of DeepSeek-R1-Distill-Qwen-1.5B using CoT on AQuA.